University of Alberta

Novel Alterations of Morphology and Genome of Mitochondria of Cholangiocellular Carcinoma

by

Wesam Ahmad Bahitham

A thesis submitted to the Faculty of Graduate Studies and Research
in partial fulfillment of the requirements for the degree of

Master of Science

in

Medical Sciences- Laboratory Medicine and Pathology

Spring 2013
Edmonton, Alberta

ABSTRACT

Cholangiocellular carcinoma (CCA) is the second most common hepatic malignancy, but its carcinogenesis is poorly understood. Somatic mitochondrial DNA (mtDNA) mutations have been demonstrated in a variety of human cancers. However, no study has previously investigated mitochondria and their genome alterations in CCA.

Our findings suggest that mtDNA alterations are an important event during the carcinogenesis of CCA. In comparison with normal cell lines and other liver malignancies, both morphologic and functional changes of mitochondria and mitochondrial genome point to a striking result that may play a major role in the aggressiveness of CCA.

ACKNOWLEDGEMENTS

I wish to express my sincere and gratitude to the following individuals without whom this thesis would do not have been possible:

To my supervisor, Dr. Consolato Sergi, for his guidance, support, patience and knowledge. He has been an incredible mentor. His balanced approach of allowing me the freedom to explore my ideas while ensuring that I stayed on track has helped me grow as a scientist. I am proud to be one of the students graduating from his lab.

My deepest appreciation is extended to my committee members, Dr. Fiona Bamforth and Dr. Alicia Chan, for their guidance and valuable support. I would also like to express my gratitude to my external examiner, Dr. Urmila Basu for reviewing my thesis and providing constructive feedback.

Dr. Sergi's laboratory has been a wonderful place to work and learn. I thank all present members of Dr. Sergi's lab for facilitating the achievement of my MSc. My graduate experience would have been incomplete without my extraordinary colleagues in the Laboratory Medicine and Pathology and Oncology Departments: Yasser Abuetabh, Redha Albhrani, Nikolas Zetouni, Oindrila Mukherjee, Indrani Dutta, Shyambabu Chaurasiya, Nour Mousaa, Ben Bablitz and Teresa Paonessa.

I would like to thank the Ministry of Higher Education in Saudi Arabia for financially supporting me during my MSc studies.

Most importantly, I thank my family for their unconditional love, support and optimism and for standing by me through all steps of my life. In particular, my great thanks to my brother Wael Bahitham for his moral support, patience and love through this wonderful experience. I dedicate this dissertation to my parents, who have shaped me into being the woman I strive to be and taught me the meaning of dedication to work as well as good morals in life.

TABLE OF CONTENTS

LIST OF TABLES

LIST OF FIGURES

LIST OF ABBREVIATIONS

APAF1	Apoptotic protease activating factor 1
ATP	Adenosine triphosphate
Atg	Autophagy related proteins
BER	Base excision repair
BNGE	Blue negative gel electrophoresis
ANT1	Adenine nucleotide translocator 1
BCSL1	Cytochrome *b–c* complex assembly protein
∆PH	Chemical potential
CA 19-9	Carbohydrate antigen 19-9
CCA	Cholangiocarcinoma/ Cholangiocellular Carcinoma
CEA	Carcinoembryonic antigen
CoQ10	Coenzyme Q10
Complex I	NADH dehydrogenase
Complex II	Succinate:ubiquinone oxidoreductase
Complex III	Ubiquinol:ferricytochrome c oxidoreductase
CIV	Cytochrome c oxidoreductase
CLL	Chronic lymphocytic leukemia
COX	Cytochrome *c* oxidase
CSB	Conserved sequence block
C-tract	Poly C-stretch
DCA	Dichloroacetate
D-loop	Displacement loop

$\Delta \mu^{H+}$	Electrical potential
ERC	Endoscopic retrograde cholangiography
FMN	Flavin mononucleotide
5FU	5 Fluorouracil
GP_X	Glutathione peroxidase
GRed	Glutathione reductase.
GRACILE	Growth retardation aminoaciduria irons overload lactic, acidosis, early death
HIF-1	Hypoxia induced factor 1
HMG	High mobility domains
HNSCC	Head and neck squamous cell carcinoma
H- strand	Heavy strand
H_2O_2	Hydrogen peroxide
IAPs	Inhibitor of apoptotic proteins
ICAD	Inhibitor of caspase activated DNase
iNOS	Inducible nitric oxide synthase
IL-6	Interleukin 6
LDHA	Lactate dehydrogenase A
L-stand	Light strand
LS	Leigh syndrome
MOM	Mitochondrial outer membrane
MOMP	Mitochondrial outer membrane permeabilization
MPT	Mitochondrial transition permeability
MRCP	Magnetic resonance cholangio-pancreatogram

mtDNA	Mitochondrial DNA
MtTFA	Transcription factor A
MtFAM	Transcription factor for termination
mETC	Mitochondrial electron transport chain
MILS	Maternally inherited Leigh syndrome
mRNA	Messenger ribonucleic acid
MRP	Mitochondrial RNA processing
NARP	Neuropathy ataxia retinitis pigmentosa
ND	NADH dehydrogenase
nDNA	Nuclear DNA
NDUF	NADH dehydrogenase-ubiquinone oxidoreductase
O_H	Origin of replication of H-strand
O_L	Origin of replication of L-strand
OGG-1	8-Oxoguanine glycosylase
OXPHOS	Oxidative phosphorylation
8-oxoG	8-oxo7,8-dihydroguanine
PCR	Polymerase chain reaction
PDKs	Pyruvate dehydrogenase kinases
PFK	Phosphofructokinase
POLG	Polymerase subunit gamma
PSC	Primary sclerosing cholangitis
PTC	Percutaneous transhepatic cholecystostomy
Q	Ubiquinol

QH_2	Ubiquinone
RC	Respiratory chain
ROS	Reactive oxygen species
RRFs	Ragged red fibers
rRNA	Ribosomal ribonucleic acid
RNOS	Reactive nitrogen oxide species
RIBA	Radioimmunoprecipitation assay buffer assay
TAS	Termination associated sequence
TCA	Tricarboxylic acid
TTBS	Tris-buffered saline
TIM	Translocases of the outer membrane
TOM	Translocases of the inner membrane
tRNA	Transfer ribonucleic acid
TTGE	Temporal temperature gradient electrophoresis
UDG	Uracil DNA glycosylase
SDHA	Succinate dehydrogenase A
SNHL	Non-syndromic and aminoglycoside-induced sensorineural hearing loss
SOD	Superoxide dismutase
VDAC	Voltage dependent anion-selective channel

Chapter 1 Introduction

Mitochondria constitute a dynamic system with multiple operational functions and ubiquitous organelles in eukaryotic cells. Specifically, mitochondria fulfill the main function of synthesizing adenosine-5'-triphosphate (ATP), the universal energy of the cell, as well as performing a central role in other vital processes, including cell death programming, calcium signaling and cell cycle regulation. These organelles contain the cell's major energy-requiring and energy-producing pathways, including the urea cycle, the citric acid cycle, heme biosynthesis, cardiolipin synthesis and the β-oxidation pathway of fatty acid breakdown. The dysfunction or deregulation of these cellular activities may cause pathological implications that result in disease, cancer, aging and lethality. Consequently, a comprehensive detailed analysis of mitochondrial molecular biology may improve the prognosis, treatment and prevention of numerous diseases.

1. Mitochondrial pathways

1.1 Mitochondrial structural overview

The name “mitochondria” was established in 1898 by Benda; this term derived from the Greek words *mitos* (thread) and *chondros* (granule) (1). In 1900, Michaelis discovered the first stain for mitochondria, known as the Redox Janus Green B, which persisted as the primary staining method until 1952 (2). Subsequently, in 1952 Palade clearly observed the cristae and double membranes by using electron micrographs. In particular, he observed that cristae constituted inward folding of the inner membrane (2). The number of mitochondria present in

a cell depends on the metabolic requirements of that cell or tissue. In fact, some cells contain only very few mitochondria, while other cells have thousands of mitochondria (3).

Recently, the fundamental understanding of the mitochondrial ultrastructure is based on sophisticated techniques that use high-resolution 3D images acquired by a high voltage electron microscopes and electron tomography scan. The elaborate structure of mitochondria is composed of two parts, which constitute highly concentrated phospholipids and proteins. These chemicals are involved in the translocation of other proteins, known as Translocases of the Inner Membrane (TIM) and Translocases of the Outer Membrane (TOM) (4). The outer membrane is permeable for large molecules and ions (mw<5000), which can diffuse easily through special channels known as porins. However, the inner membrane, which prevents most molecules from passing through the mitochondria, is more selective than the outer membrane. In addition, the inner membrane contains the respiratory chain complexes and the matrix. The matrix is encircled by the inner mitochondrial membrane involved in the citric acid cycle enzymes, which are responsible for reducing acetyl CoA to CO_2. During this process, electrons that are released enter the respiratory chain complexes and reduce these complexes to molecules of H_2O and ATP, which is the fuel of the cell. Recent research examining the cristae demonstrates that these components not only represent the folding of the inner membrane but also function as an internal compartment created by the membrane invagination (5). In addition, current evidence suggests that the specific morphology of the cristae may regulate

parts of the apoptotic pathway, eradicate diffusion of ATP production and provide resistance to oxidative stress (5).

1.2 Mitochondrial genome (mtDNA) overview

The differentiation of the mitochondrial genome from the nuclear genome was observed in the late 1950s and early 1960s (6). Early revelations illustrated that mitochondrial DNA contained a separate protein structure that could synthesize the mitochondrial ribosome components, rRNA and tRNA. Subsequent steps investigated mitochondrial DNA in yeast and in other organisms. Remarkably, the results of these studies established a distinct structure and gene organization of mtDNA (6). The first complete mtDNA genome was obtained from the human species, and the sequence of mammalian mtDNA has been recorded in the MITOMAP database, which is an open source (www.mitomap.org) available to all researchers investigating mitochondria (7). In 1981, Anderson *et al*. reported the analysis of human mtDNA sequence, specifically the gene arrangement, gene expression and coding capacity (Figure 1.1) (8).

Mammalian mtDNA includes genes for 13 protein subunits of respiratory chain complexes, including seven subunits of complex I, one subunit of complex III, three subunits of complex IV and two subunits of complex V. In addition, mammalian mtDNA harbors genes for both 22 tRNA and 2 rRNA (Figure 1.2). MtDNA is considered as a prototype since its structure and genetic organization is strongly conserved in other mammals (9). Specifically, human mtDNA is a closed-circular and double-stranded DNA molecule of approximately 16.6 kb. The

double strands of mtDNA are distinguished by their G+T content, which results in a heavy strand, or H-strand, and a light strand, or L-strand (Figure 1.1). The vast majority of genes encoded by mtDNA exist on the heavy (H) strand, with genes for 2 rRNA, 14 tRNA and 13 proteins in different complexes. However, eight tRNA and a single polypeptide, which are encoded by mtDNA, occur on the light (L) strand (Figure 1.1)(8,10).

There are two noncoding regions in the mtDNA that contain the vast majority of its known regulatory functions (11,12). The main region is known as the displacement loop, or D-loop, which occurs on the nascent H-strand that is formed in this region. Specifically, the D-loop is located between the genes for $tRNA^{Phe}$ and $tRNA^{Pro}$, which contain the origin of replication for the H and L strands (O_H) and the bi-directional promoters. The D-loop structure primarily consists of conserved sequences known as CSB_S or "conserved sequence blocks", TASs "termination–associated sequence" and tRNA, which fulfills a pivotal role in mtDNA replication (6,12,13). The second non-coding region is 30 nucleotides long and is located approximately two-thirds of the mtDNA length from O_H. It involves the origin of replication for the L-strand (O_L) (12).

1.2.1 Mitochondrial DNA versus nuclear DNA

There are unique features of mtDNA that genetically distinguish it from nuclear DNA (nDNA). First, each human cell contains hundreds of mitochondria, each of which possesses 2-10 copies of mtDNA. While homoplasmic mtDNA consist solely of identical copies in an individual cell, heteroplasmic mtDNA

contain copies that are not identical in either mutant or wild species (6,10). In order to exhibit pathological presentations, at least 60-70% of mtDNA must contain mutant copies, a phenomenon labeled as the “threshold effect”. Secondly, the mitochondria genome is derived from the mother. Specifically, the mother transmits her oocyte mtDNA to her progeny, and only her daughters can transmit their mtDNA to the next offspring (14). Study by Giles et al., suggested that while a few mitochondria sperm could enter the zygote, these sperms will eventually be destroyed by an ubquitin–dependent mechanism during fertilization (14). Furthermore, the evolution rate of mtDNA is much faster than that of nDNA, as mtDNA is protected neither by histone nor chromatin. As a result, mtDNA likely incur more damage by reactive oxygen species (ROS) inside the inner membrane of the mitochondria, where ROS are generated (15,16). Hence, since mitochondria lack an effective repair system, the high mutational rate and maternal inheritance mode has been an object of investigation for a role in aging and cancer (12).

1.3 Mitochondrial function overview

The mitochondria are described as the "cell’s power" because they generate most of the cell energy supply by converting oxygen and nutrients in presence of oxygen into adenosine triphosphate (ATP). In addition to producing energy, mitochondria are responsible for biochemical synthesis, calcium storage, metabolic detoxification and programmed cell death or apoptosis.

1.3.1 Respiratory chain complexes

The operational structure of oxidative phosphorylation (OXPHOS) system comprises two sets of reactions. The first reaction is constituted by the respiration, consisting of O_2 consumption that is conducted by electrons in the first four respiratory chain complexes. These complexes include CI, NADH (ubiquinone oxidoreductase), CII (Succinate: ubiquinone oxidoreductase), CIII (ubiquinol: ferricytochrome c oxidoreductase) and IV (cytochrome c oxidoreductase). The resulting oxygen molecules are ultimately reduced to water. During this process, the second reaction, the production of ATP synthase by electrochemical proton gradients occurs. ATP synthase represents the second set of OXPHOS (Complex V), which generates ATP (Figure 1.2) (17,18).

Complex I is considered as the largest of all complexes in the OXPHOS system. This complex constitutes 45 subunits, 7 of which are encoded by mtDNA, while 38 subunits are encoded by nDNA (19). The crystallization structure of CI, which can be ascertained in a low-resolution 3D electron microscope, exhibits an L-shape with two arms. While the longer arm is located in the matrix, which is more negative, or hydrophilic, the short arm extends into the membrane, which is more positive, or hydrophobic (20). These structures have three main functions. First, two electrons are transferred from NADH and subsequently passed through FMN, which contains flavoprotein, to a series of at least six Fe-S centers that are located in the matrix. The reduction of ubiquinone coenzyme Q10 (CoQ) to ubisemiquinone and then to ubiquinole in the membrane works as a hydrogenase, which contains a significantly negative charge. During this process, the net

transfer of four protons is translocated from the matrix to the inner membrane space, creating a unique proton gradient that will be used to generate the ATP proton translocation function (6,21). Each structural subunit of CI fulfills an essential role in its stability and assembly. In particular, the mutation of *ND2* causes an accumulation of the CI intermediates. The mutations of *ND1*, *ND4*, and *ND6* are associated with the down-regulation of the CI enzymes, because these parts are essential for CI assembly. However, the mutations of *ND3* and *ND5* are not essential for the enzymatic activity of the CI assembly (15,16).

Horton et al. reported the first significant mtDNA mutation in cancer, which involved the deletion of 294 nucleotides in *ND1* in patients with renal adenocarcinoma (22). Specifically, these authors demonstrated that transmitochondrial cells harboring the T14487C mutation in *ND6* induced ROS production (23). Research has illustrated the role of mitochondrial mutations in Complex I during the progression of tumor metastasis in mouse tumor cell lines with high or low metastatic potential. While a large number of metastatic cells demonstrated a reduction in Complex I activity, a small number of these cells did not result in any such change (24).

Complex II is the simplest of the RC complexes. Composed of four nDNA-encoded subunits, this complex has not appeared to form super-complexes with other electron transport chain (ETC) components (25,26). The electrons reach the ubiquinol via iron-sulfur centers (Fe-S) and flavin adenine dinucleotide (FAD). Since this process does not involve the presence of a proton pump, this

complex does not contribute to the energetic potential for synthesizing ATP (25,26).

Complex III contains 11 subunits in which cytochrome *b* is encoded by mtDNA; however, the other eight subunits are encoded by nDNA. The net reaction of this complex oxidizes two molecules of QH_2 (ubiquinone) to Q (ubiquinol) by producing two protons per one molecule of Q, for a total of four molecules and one electron per two protons, which are then transferred to CIV. While one proton relocates to cytochrome c_1 in the inner membrane space, the other one migrates to the Q site to undergo reduction to QH_2 in the matrix (27).

Since cytochrome *b* may incorporate enzymatically with CI supercomplexes, this subunit is associated with a CI+CIII deficiency. Some studies report that more than 20 pathogenic mutations are associated with the CIII assembly factor, BCS1L. Various clinical phenotypes are likely associated with BCS1L mutations, which include the multi-visceral GRACILE syndrome (growth, retardation, aminoaciduria, cholestasis, iron overload, lactic acidosis and early death) to congenital metabolic acidosis, neonatal proximal tubulopathy, liver failure and encephalopathy (28).

Murine and human urothelial carcinoma/ transformed cells experienced a 21bp deletion of mitochondria-encoded cytochrome *c*, which resulted in increased ROS, lactate production and oxygen consumption (29). Also, murine and human bladder cancer models have shown invasive phenotypes that are able to destroy normal splenocytes, thus indicating the ability of mutant cells to promote tumor growth and subsequently evade the immune system surveillance (29).

Complex IV, the terminal enzyme of the ETC, is composed of 13 subunits. Three of these subunits, MTCO1, MTCO2 and MTCO3, are encoded by mtDNA while the other ten subunits, COX4, COX5A, COX5B, COX6A, COX6B, COX6C, COX7A, COX7B, COX7C and COX8, are encoded by nDNA (30,31). This complex is located in the region where electrons are transferred from the cytochrome *c* to molecular O_2 and then reduced to water. CIV is catalyzed by specific keys: subunit I and subunit II (30). During the catalyzing process, electrons pass from cytochrome *c* to O_2 through subunit II, which is contained in the first binuclear center or Cu_A. Afterwards, the electron migrates from heme a to heme a_3 (Subunit I), which forms the second binuclear center with the copper ion or Cu_B (31). This enzyme comprises two proton input channels: the D-channel and the K-channel (32). Although the D-channel pumps four protons per O_2, it only supplies two of the four protons that are required for the reduction of O_2 (32,33). The K-channel is not directly used for the uptake of pumped protons; however, it provides the remaining protons for the active site of O_2 (33). Therefore, the oxygen binds to the Cu_B center, and the net of four electrons passes from cytochrome *c*; the cytochrome *c* oxidase will use the substrate H^+ from the matrix to convert O_2 to H_2O (6,33-35).

COX deficiency is a major cause of mitochondrial diseases in human pathology and is also associated with various clinical presentations. CIV biogenesis requires multiple proteins that are involved in the protein assembly process but are not necessarily involved in the maturation of the enzyme (6,34). For instance, Sufr1 is involved in the COX assembly, and mutations in this gene

are responsible for causing Leigh syndrome with COX deficiency (LS^{COX}). Furthermore, COX10 and COX15 are essential enzymes for the catalytic center of CIV, which is incorporated during the terminal step of the heme a biosynthetic pathway. COX10 mutations are associated with leukodystrophy and renal tubulopathy (36) while COX15 mutations are related to Leigh syndrome and fatal infantile hypertrophic cardiomyopathy. Mutations of these enzymes are relatively rare in humans. Mutations of SCO1 and SCO2 genes, which are responsible for inserting copper into the catalytic center, are associated with fatal infantile hepatic failure and infantile cardiomyopathy respectively (37).

Interestingly, defects in the cytochrome *c* oxidase leading to increased ROS levels and mtDNA damage have been reported in cancers (38-40). Similarly, the low expression of COXII and the high expression of COXI and COXIII have been associated with various cancers (39-42).

1.3.2 Oxidative phosphorylation

Complex V (ATP synthase): According to the chemiosmotic hypothesis, the protons that are pumped by the electron transport chain across the inner mitochondria membrane through CI, CIII and CIV should create a proton electrochemical gradient that includes electrical potential ($\Delta\boldsymbol{\mu}^{\mathbf{H+}}$) and chemical potential (ΔPH). The mitochondrial membrane potential ($\Delta\psi$) averages between -180 to -250mV. Through oxidative phosphorylation, the electrochemical gradient is used by F_0-F_1 ATP synthase to produce ATP (Figure 1.2). The energy converts ADP + Pi to ATP by F_0-F_1, which acts as ion channels, allowing the translocation

of protons from the inter membrane back into the matrix (43,44). The mitochondrial membrane potential is dependent on superoxide production and recruitment of the mitochondrial uncoupling proteins, corresponding to a depolarization of only 20-30mV (43,44).

Most of the CV mutations are intensively concentrated in the *MTATP6* gene. In particular, the main clinical presentations related to transversion 8993T>G and transition 8993T>C in the *MTATP6* gene include NARP (neuropathy, ataxia and retinitis pigmentosa) and severe infantile MILS (maternally inherited Leigh syndrome) (45,46). Also, the alteration of *ATP6* has been associated with prostate cancer (47). Rodents tumors harboring *ATP6* with 8993T>G mutation-producing ROS eventually result in DNA damage and tumor growth (41). Furthermore, HeLa cell hybrids containing *ATP6* with 8993T>G and 9176T>C exhibit decreased mitochondrial respiration and accelerated tumor growth by prevention of apoptosis (48).

1.3.3 Generation of reactive oxygen species

Mitochondria are metabolized to form ROS under normal physiological conditions, and thus, these organelles are considered as a major site of ROS, which are generated through the ETC (49). Two main factors determine the rate of mitochondrial superoxide formation: electron influx and oxygen concentration (50-52). The electron leak from ETC is mainly present in CI and CIII. In CIII, the Q-cycle is the major site of oxygen reduction, which occurs as a result of the reaction between molecular oxygen and ubisemiquinone in the matrix and the

inner mitochondrial membrane (50-52). Eventually, most of the superoxide is converted into hydrogen peroxide (H_2O_2) by two different superoxide dismutases (SOD); however, part of the superoxide will react with cytochrome *c* and subsequently undergo reoxidation to molecular oxygen, thus contributing to ATP production (53,54). During this process, H_2O_2 can undergo Fenton chemistry to form the highly-reactive hydroxyl radical (55-57). On the other hand, CI has many proposed redox centers for producing ROS, including two iron-sulfur centers as well as FMN, the prosthetic group of NADH-dehydrogenase; however, it is not yet clear which redox center is responsible for releasing ROS in CI (58,59).

At standard cellular levels, ROS fulfills essential roles in cell signaling for a normal cellular functionality. However, an excess of ROS can cause damage to cellular components, including proteins, lipids and DNA (60). In cancer cells, the exposure to a hypoxic environment enhances obviously mitochondrial ROS production. Thus, the cells activate the adaptation mechanism of the hypoxic condition, including transcription factor hypoxia-inducible factor 1 (HIF-1), which is a key mediator of the hypoxia response through regulating genes involved in metabolism, angiogenesis, cell cycle and apoptosis (49,61). HIF-1 also activates the pyruvate dehydrogenase kinases (PDKs), which disable the mitochondrial pyruvate dehydrogenase complex, consequently decreasing the flow of glucose-derived pyruvate into the tricarboxylic acid (TCA) cycle (62, 63,64). The reduction of pyruvate in the TCA cycle reduces the rate of oxidative phosphorylation and oxygen consumption, strengthening the glycolytic phenotype and preserving oxygen under hypoxic conditions.

In addition, the oncogenic transcription factor MYC impacts cell metabolism in several ways (65,66). During the process of glycolysis, highly-expressed oncogenic MYC, along with HIF, participates in the activation of several glucose transporters and glycolytic enzymes as well as lactate dehydrogenase A (LDHA) and PDK1 (66,67). However, MYC also activates the transcription of targets that increase biogenesis and the function of mitochondria (66,67).

Another important contributor to ROS production in cancer cells involves p66shc, which has been implicated in carcinogenesis. Recently, it has been postulated that p66shc increases mitochondrial oxidative stress by negatively regulating manganese-superoxide dismutase II (SODII) (68,69). Moreover, research has shown that fibroblast null p66shc resists ROS-induced apoptosis in p53 and has downstream effects on this protein. In cancer, increased oxidative stress not only contributes to metabolic disturbances by HIF1 but also activates the malignant phenotype by promoting several survival pathways (70).

ROS can cause damage to different cellular components, including mtDNA. In fact, ROS molecules are highly active and diffusible. The use of antioxidants as a primary defense against ROS has both enzymatic and non-enzymatic components (71). Enzymatic components include manganese superoxide dismutase (SODII), glutathione peroxidase (GP_x), glutathione reductase (GRed), peroxidase, glutaredoxins and proteins, such as cytochrome *c*. On the other hand, non-enzymatic elements include reduced glutathione (GSH) and a high NAD (P)H/NAD(P) ratio (72). While hydrogen peroxide is detoxified

into water and oxygen by catalase, other hydroperoxides are detoxified by glutathione peroxidase (GP_x) in the mitochondria and in the cytosol. All of these antioxidants have been altered in tumor cells as compared with their corresponding normal tissues. In fact, cancer cells have been found to be deficient in antioxidant enzymes (73).

1.3.4 Apoptosis

Apoptosis, or programmed cell death, is mediated by a series of caspases, leading to energy-dependent cell death. Cell death was initially described by its morphological characteristics, including cell shrinkage, membrane destruction, chromatin condensation and nuclear fragmentation (74-76). Two main apoptotic pathways have been identified: intrinsic and extrinsic (Figure 1.3) (77). Both of these pathways can cause the mitochondrial translocation of pro-apoptotic (Bcl-10, Bax, Bak, Bid, Bad, Bim, Bik) and anti-apoptotic (Bcl-2, Bcl-x, Bcl-XL, Bcl-XS, BAG) members of the Bcl-2 family in the outer mitochondrial membrane, thus resulting in mitochondrial outer membrane permeabilization (MOMP) (78-80).

The protein p53 promotes apoptosis by the expression of several downstream target genes that specify the apoptotic machinery. Specifically, while p53 encodes the genes of the pro-apoptotic proteins, it represses the expression of genes specifying anti-apoptotic proteins (81,82).

The extrinsic pathway for apoptosis can be triggered by cell surface receptor death (Figure 1.3). In particular, many signals activate the intrinsic pathway by

mediating the mitochondrial transition permeability (MPT), including oxidative stress, temperature stress, toxins, radiation, calcium overload and impaired electron transport chain (83,84). When these signals initiate this pathway, the outer membrane becomes depolarized, thus losing its mitochondrial membrane potential, and cytochrome *c*, Smac/DIABLO (Second mitochondria-derived activator of caspase/direct inhibitor of apoptosis-binding protein) and HtrA2 (high temperature requirement protein A2) are released from the mitochondria and into the cytosol (85). Specifically, cytochrome *c* combines with Apaf-1 (apoptotic protease activating factor) to form apoptosome, which activates procaspase 9 into caspase 9 (86). Subsequently, caspase 9 activates procaspase 3 into caspase 3, an executioner caspase (77). In addition to cytochrome *c*, Smac/DIABLO (second mitochondria derived activator of caspases) is released to inactivate the inhibitors of apoptotic proteins (IAPs). These IAPs can either directly to inhibit the activity of protolytic caspases or they can label caspases for ubiquitination and degradation in order to block caspase action (Figure 1.3) (87).

The executioner caspases, including 3, 6 and 7, destroy the critical components of the cells by cleaving the inner surface of the nuclear membrane (lamin) as well as the cytoskeleton proteins (actin, plectin, vimentin and gelsolin) and inhibiting caspase-activated DNase (ICAD). Each of these actions results in the final morphological hallmarks of the apoptotic program (Figure 1.3) (74-76).

1.4 The role of mitochondria in cancer

Frequent mtDNA mutations have been reported in different stages of cancer progression, suggesting that a functionally significant correlation between

mtDNA mutations and depletion may indicate tumorigenesis. Mitochondrial mutations are essentially homoplasmic in nature. This event may implicate that mtDNA is a potential molecular substrate involved in cancer promotion or proliferation. Research data evidence that in comparison to normal cells, tumor cells have lower mtDNA content. Recently, rapid and high-throughput sequencing have been developed to detect mtDNA sequence variants in patient cancer samples. Therefore, experimental approaches represent a promising tool for discovering the link between mtDNA variants and tumorigenesis, or mtDNA alteration and tumor proliferation or growth.

1.4.1 Warburg effect

Cells can produce energy through oxygen-dependent (aerobic) pathways of oxidative phosphorylation (OXPHOS) and through the oxygen-independent process of glycolysis. Under normoxic conditions, cells rely on aerobic respiration (OXPHOS) to generate energy via the oxidation of glucose, fatty acids and amino acids in cytosolic and mitochondrial processes. In aerobic respiration, glucose is partially oxidized to pyruvate in the cytosol. Pyruvate is then imported into the mitochondria, where it is fully oxidized through two sets of reactions: tricarboxylic acid (TCA) and oxidative phosphorylation (OXPHOS), where the electrons resulting from the oxidation of NADH and $FADH_2$ require acceptance by oxygen (Figure 1.4). However, when oxygen levels are low, cells rely on glycolysis and subsequent lactic acid fermentation, which occurs in the cytosol. In this process, glucose is converted to pyruvate, which is converted to lactate by

NADH rather than transported into mitochondria. In comparison to glycolysis, OXPHOS is more efficient in producing ATP. In fact, one molecule of glucose results in 2 ATP molecules during glycolysis and up to 36 ATP molecules through the OXPHOS reaction (34,88) (Figure 1.4).

In the 19th century, Pasteur observed that low levels of O_2 caused the generation of ATP shifted from OXPHOS to glycolysis, a phenomenon known as the Pasteur Effect (89). One century later, Otto Warburg used living tissue to observe that normal cells use glycolysis only in the absence of oxygen whereas tumor cells exhibit an increased rate of glycolysis under normal aerobic conditions. In addition, he proposed that due to an irreversible defect in OXPHOS, cancer cells demonstrate an increased glycolytic rate despite the presence of O_2 levels. This phenomenon, known as the Warburg Effect, was initially rejected (90). One possible explanation for this hypothesis involves the fact that most common cancer types exhibit a decreased expression of ATP synthase, a protein complex required for OXPHOS. Consequently, cells that are deficient in ATP often undergo apoptosis. Moreover, it has been shown that mitochondrial mutations lead to OXPHOS dysfunctions in tumor cells and facilitate the inactivation of p53(91). However, the Warburg Effect has also been observed in non-transformed proliferating cells, which are not supposed to incur to irreversible damage to OXPHOS. This evidence has been recently supported by the hypothesis that cancer cell can enhance OXPHOS in the case that glycolysis is inhibited, thus indicating that the Warburg Effect is not only caused by irreversible damage to OXPHOS (92-94).

Recent studies suggest that cancer cells contain alterations in O_2 metabolism, which may contribute to tumor growth, invasion and metastasis as well as fulfilling a function in the Warburg Effect. Cells control the activation of glycolysis by reducing the metabolism of O_2 through OXPHOS. A low level of O_2 metabolism will ultimately decrease the rate of ATP generation, which enhances the release of phosphofructokinase (PFK), a key enzyme in the regulation of glycolysis, resulting in glycolysis activation. Therefore, a decrease in O_2 metabolism via OXPHOS can activate glycolysis. However, a high level of O_2 metabolism through ROS ($O_2^{\cdot-}$ and H_2O_2) may also produce glycolysis. $O_2^{\cdot-}$ produces intracellular alkalization (↑pH), which enhances glycolysis by increasing the activity of PFK (95,96). It has been shown that H_2O_2 can activate HIF-1(97,98), which performs a role in the transcription genes for glucose transporters and glycolytic enzymes (99,100).

Cancer cells activate glycolysis by alterations in O_2 metabolism involving OXPHOS repression, increased generation of $O_2^{\cdot-}$(101) and H_2O_2 (102,103), intracellular alkalization (104,105,106) and HIF-1 stimulation (99). All of these factors have been experimentally demonstrated in most cancers containing structural alterations in OXPHOS (91,107) as well as the excessive generation of $O_2^{\cdot-}$ (101) and H_2O_2 (102,103), which may lead to OXPHOS repression.

1.4.2. mtDNA mutations in cancers

As a result of their proximity to the ROS generation site, mitochondria contain a relatively unsophisticated DNA repair system (108,109). While neutral

polymorphisms are most likely homoplasmic, pathogenic mutations are usually considered heteroplasmic. Due to the multiplication process of the mitochondrial genome, the mutation threshold is reached when a minimal critical number of mutant mtDNA are present, causing mitochondrial dysfunction in one or more organs or tissues (108,109). Using the electron microscope, Clyton and Vinograd reported the first indication of mtDNA in the leukocytes of human leukemia (110). Alterations in the restriction pattern of the mtDNA have been reported in renal carcinomas (22) and breast tumors (111) based on restriction enzyme analysis. Moreover, it was proposed that in the D-loop region, a poly C-stretch (C-tract) is more susceptible to oxidative damage and electrophilic attack as compared with other regions of mtDNA (112). While most of the previous studies focused on the analysis of the non-coding D-loop region, a somatic 50-bp mitochondrial D-loop deletion has been detected in gastric adenocarcinoma (113). Frequent mutations within the D-loop region have also been reported in ovarian, gastric and hepatocelluar carcinoma (114,115,116).

Subsequent studies have identified the mutations in coding and non-coding regions of mtDNA in different types of human cancers; most of these mutations appeared to be homoplasmic (117,118). Systematic analyses reviewed 101 papers published between 1998 and 2008 by performing Medline searches with “mtDNA” “mutation” and “cancer/tumor” as keywords. The majority of these mutations (635) were found in the D-loop region (119). In addition, 593 mutations were reported in genes encoding Complex I with frequency of 9.3% as compared with other respiratory complexes (119). A high level of mutations have

been also reported in tRNA and rRNA genes; in the majority of cases, these mutations are associated with multisystem disorders, lactic acidosis, and mitochondrial proliferation, which results in the ‘‘ragged-red’’ appearance of muscle fibers (120-123) with the modified Gomori trichrome stain. Comprehensive mutational analysis of the entire mitochondrial genome have been accomplished by direct sequencing (124), Temporal Temperature Gradient Electrophoresis (TTGE) (125) and MitoChip analysis (126). The entire mitochondrial genome was sequenced in 10 colon cancer cell lines (127). Seventy percent of the cell lines exhibited a total of 12 mtDNA mutations, which were found in rRNA (12S and 16S) as well as in subunits of Complex I (*ND1*, *ND4L* and *ND5*), Complex III (cytochrome *b*) and Complex IV (*COX I*, *COX II* and *COX III*). In particular, all of these mutations were somatic mutations that were not detected in the primary tumors from which the cell lines were derived (127). However, another complete sequencing of the mitochondrial genome revealed a high level of mtDNA mutations in normal colonic crypt stem cells (128), which indicates that such mutations actually occur prior to the development of colon cancer. Nevertheless, research has not yet established whether these mutations actually cause malignancy (128). Several studies of mtDNA sequence variants using a whole genome approach were reported in various cancers, including bladder (129), breast (130,131), esophagus (130), head and neck (132,133), leukemia (134,135), lung and thyroid gland (38,136,137). The majority of these human cancers (129-133,138) involve the frequency of somatic mtDNA mutations, which are mainly homoplasmic with low levels of heteroplasmy.

The contribution of mtDNA mutations and mitochondrial dysfunction in tumorigenesis has recently been studied using human cell lines harboring a frame-shift mutation in the Complex I, subunit 5 gene. As a result of increasing mutant *ND5* content, respiratory functions, including oxygen consumption and ATP generation, were decreased, while lactate production and dependence on glucose were elevated (127). Significant tumor growth was demonstrated in the cell line harboring heteroplasmic *ND5* mtDNA mutation; however, the growth was inhibited in the cell line with a homoplasmic *ND5* mtDNA mutation (127). In another study, the pathogenic mtDNA *ATP6* T8993G mutation in the PC3 prostate cancer cell line through hybrid transfer was tested for tumor growth in nude mice (48). The resulting mutant (T8993G) hybrids were found to generate tumors that were seven times larger than the wild-type (T8993T) hybrids (61). The contribution of mtDNA to tumor cell metastasis was investigated, demonstrating that G13997A and 13885insC in the *ND6* gene promoted the highest metastatic potential in mtDNA variants (24).

1.4.3 MtDNA copy number

In addition to mtDNA mutations and deletions, alterations in the mtDNA copy number have been studied in various tumor types. A decrease in mtDNA content has been reported in breast (139) renal (140), hepatocellular (141) and gastric cancer (142). It has been demonstrated that reduced mtDNA leads to increase invasiveness and aggressiveness of the cancer (143). Conversely, an increase in the mtDNA copy number has been reported in head and neck

squamous cell carcinoma (144), papillary thyroid carcinoma (139,145) and lung cancer (146). Furthermore, this increase has also been associated with chronic lymphocytic leukemia (CLL), Burkett lymphoma, Epstein-Barr virus–transformed lymphoblastoid cell lines, non-Hodgkin's lymphoma and small lymphocytic lymphoma (147). Hence, an altered mtDNA copy number has been suggested as a compensatory mechanism for mtDNA damage (144). This alteration depends on several factors, including the site of mutation in the mitochondrial genome, such as the D-loop region, which is involved in mtDNA replication and transcription, leading to the depletion of mtDNA content (144).

1.4.4 Mitochondria as targets for cancer therapy

Recently, mitochondria in cancer cells have emerged as an obstacle to for tumor destruction. Anti-cancer agents that specifically target cancer cell mitochondria are referred to as 'mitocans'. The mechanism of action for mitochondrial targeted anti-cancer drugs depends on their ability to disrupt the energy-producing systems of cancer cell mitochondria, leading to the elevated formation and accumulation of ROS, which, in turn, induces the intrinsic, mitochondria-dependent pro-apoptotic pathways (148). Based on their mode of action, mitocans have been classified into individual groups acting on targets, including the cytosolic face of the mitochondrial outer membrane (MOM) and targets within the mitochondrial matrix.

Accordingly, other options include dichloroacetate (DCA), which enhances the activity of pyruvate dehydrogenase kinase inhibitor, shifting the

metabolism of the cell from glycolysis to glucose oxidation, which leads to a decrease in tumor growth and increases of cell apoptosis. While the DCA has a side effect on normal cells, it selectively kills the cancer cells that rely on glycolysis (149).

Future research may provide evidence for the benefits of these compounds, potentially leading to the development of clinically relevant drugs that will assist in managing numerous neoplastic diseases.

1.5 Hepatobiliary carcinoma

1.5.1 Hepatocellular carcinoma

Hepatocellular carcinoma (HCC) constitutes an aggressive primary liver tumor that arises from the hepatocytes, which is the major cell type in the liver. HCC accounts for 80%-90% of primary liver cancer (150) and comprises the fifth most common cancer variety worldwide (151). The incidence of HCC depends upon the geographical zone. Hepatitis B virus (HBV) is the cause for the highest incidences of HCC in Africa and Southern Asia (152). In fact, the most crucial risk factors for HCC include chronic hepatitis virus infections (HBV and HCV) and aflatoxin-B1 (152,153). In 80% of cases, the pathophysiological process preceding malignancy that is detected in this disease is cirrhosis (152). Other diseases are also correlated with HCC development, such as iron overload (hemochromatosis) (154), deficiency of alpha-1-antitrypsin (155) and tryosinemia (156). Patients suffering from HCC have a poor prognosis and a survival rate of less than 5%. Unfortunately, there are no signs or symptoms of HCC until it reaches its

advanced stages or when the diameter of the tumor exceeds 10 cm, or compromises the liver function (152).

1.5.2 Cholangiocarcinoma

Cholangiocarcinoma (CCA) is an epithelial cancer originating from bile ducts that contain features of cholangiocyte differentiation (157-159). Next to hepatocellular carcinoma, CCA is the second most common primary hepatic malignancy. Anatomically, CAA is classified into intra-hepatic and extra-hepatic biliary systems. The extrahepatic system is further subdivided into perihilar (Klatskin) and distal extrahepatic cholangiocarcinoma based on the level of occurrence (160). According to its microscopic appearance, extrahepatic CCA displays three different growth patterns: periductal infiltrating, papillary or intraductal, and mass forming (160). Among these patterns, periductal infiltrating is the most common. On the other hand, intrahepatic CCA appears as mass forming, periductal infiltrating and intraductal (161). Histologically, most of these tumors are considered as adenocarcinoma (162).

1.5.2.1 Epidemiology of CCA

CCA accounts for less than 2% of all human malignancies and 10-15% of all primary hepatic malignancies (163). Specifically, extrahepatic CCA accounts for 80% to 90% of CCA whereas intrahepatic CCA comprises 5% to 10% of this cancer (164). Over the last three decades, the incidence of intrahepatic CCA has increased (165), while the incidence of extrahepatic CCA has remained stable

(166). However, the causes for the increased incidence of CCA have not yet been identified (167). CCA is more common in males due to the predominant occurrence of primary sclerosing cholangitis (PSC) in men (168). Moreover, there is significant geographic variability in CCA due to diverse regional environmental risk factors; in particular, there are high rates in Asia, especially Southeast Asia (168). The majority of CCA patients are middle-aged adults, most of them older than 65 years, and the cancer is rarely diagnosed in patients younger than 40 years of age (168).

1.5.2.2 Etiology of CCA

Most cases of CCA have developed without an identifiable etiology. However, certain risk factors have been established for this cancer (163). In particular, the most common risk factor associated with CCA is primary sclerosing cholangitis, with a 5% to 15% prevalence rate (169). Another risk factor entails fibropolycystic malformation of the segmental bile ducts, also known as Caroli's disease. In this condition, patients with untreated cysts face a 15-20% risk of developing CCA (170). Furthermore, hepatobiliary flukes (*Opithorchis viverrini* and *Cholorichis sinenesis*) can lead to CCA in 8-10% of cases (171). Theses flukes are endemic in Southeast Asia and Japan, where ingesting uncooked fish is common (171). Hepatolithiasis is another risk factor for CCA, as it contains a 10% incidence rate, which is more common in Asia than in Western countries (172). The exposure to chemical agents such as nitrosamines, dioxin, asbestos and thorotrast also has been correlated with an increased risk for CCA

(173,174). Regardless of the cause, cirrhosis appears to be associated with CCA; specifically, patients with hepatitis C or hepatitis B have an increased risk of developing intrahepatic CCA, although rates are different from HCC and this topic is still controversially debated in the literature (168).

1.5.2.3 Pathogenesis of CCA

The previously mentioned etiological factors lead to an environment of chronic inflammation and cholestasis, thus stimulating the biliary epithelium to be prone to malignant transformations. Chronic inflammation promotes the expression of multiple cytokines by cholangiocytes and inflammatory cells (175,176). One key cytokine in the pathogenesis of CCA is interleukin-6 (IL-6) (177), as studies have reported that CCA patients possess elevated IL-6 serum concentrations (178). Specifically, IL-6 promotes the CCA by up-regulating the anti-apoptotic protein Mcl-1 (myeloid cell leukemia-1), resulting in CCA resistance to cytotoxic therapy (179). Cytokines stimulate the expression of inducible nitric synthase (iNOS) in epithelial bile duct cells. Furthermore, enhanced iNOS activity leads to the production of nitric oxide and reactive nitrogen oxide species (RNOS) (180). These chemicals block DNA repair proteins and apoptosis through the nitrosylation of the base excision repair enzyme, 8-Oxoguanine glycosylase (OGG1), and caspase 9 (181). Studies have shown increased iNOS expression in primary sclerosing cholangitis and cholangiocarcinoma. Furthermore, iNOS has been identified in the elevated serum nitrate concentration for patients with liver fluke infection (180,181). Several oncogenic mutations, growth factors, proto-oncogenes activations and tumor

suppressor gene inhibitions have been identified in human CCA (182,183). The proto-oncogene k-ras and the tumor suppressor gene p53 are commonly mutated in malignancies; in particular, mutations of k-ras have been detected in 20% to 54% of intrahepatic CCA incidences (183). Moreover, 21.7% to 76% of CCA incidences exhibit a nuclear accumulation of p53 as well as the up-regulation of the related proteins, murine double minute (mdm-2) and cyclin-dependent kinase inhibitor 1 (WAF-1) (183,184). Research has demonstrated modifications in coding regions of adhesion molecules and anti-angiogenic factors that increase the invasion and propagation of tumors (175,185).

1.5.2.4 Laboratory tests and tumor markers for CCA

Laboratory-based analysis and diagnosis of CCA is limited to serum, bile, bile duct brush and lymph node pathology. Several markers of cholestasis, including bilirubin, alkaline phosphate and gamma glutamyltransferase, are generally increased in CCA (186,187). In particular, frequently examined serum tumor indicators include the carbohydrate antigen 19-9 (CA 19-9), carbohydrate antigen 125 (CA-125) and carcinoembryonic antigen (CEA) (188). However, two of these markers, CEA and CA-125, are relatively general; they are also elevated in other gastrointestinal malignancies and bile duct diseases, such as cholangitis and hepatolithiasis (188). Among these markers, CA 19-9 is presently the most common indicator of CCA. However, CA 19-9 possesses two major limitations; first, its serum concentration depends on the Lewis phenotype (189). Moreover, CA 19-9 is also elevated in other gastrointestinal malignancies (190,191). The

cutoff level of CA 19-9 > 129 U/mL possesses a sensitivity level of 78.6% and a specificity of 98.5%. Over time, a change in CA 19-9 registered a sensitivity of 90% and a specificity of 98% (192).

1.5.2.5 Treatment

1.5.2.5.1 Surgery

Currently, surgery is the only therapeutic option for CCA patients. Specifically, radical surgery is required in many cases, especially complete resection, which is the most effective therapy for CCA patients. Crucial criteria for resectability include factors such as the biliary tree tumor involvement, vascular invasion, hepatic lobulus atrophy and obviously metastatic disease (193). In addition, other clinical data require consideration, such as nutritional conditions and laboratory tests of serum bilirubin and albumin levels, both of which are indicators of liver failure following surgery (194). Routine imaging is necessary for evaluating metastasis, tumor location and tumor extent; such as imaging entails ultrasonography, abdominal and chest computed tomography and cholangiography. The latter category includes magnetic cholangio-pancreatogram (MRCP), percutaneous transhepatic cholangiography (PTC) and endoscopic retrograde cholangigram (ERC) (193). Although complete surgical resection remains the only curative strategy for IH- CCA, many patients with advanced stages of the disease cannot be treated through surgical management (193). Moreover, the appropriateness of performable curative surgical resection depends upon the tumor location. While recent outcomes of surgical resection have notably improved, further advancements in this field are still necessary (193). In

particular, surgical resection for IH-CCA has still exhibited a 5-year survival rate of up to 22%- 36% (195). The greatest predictor of patient survival involves tumor-free surgical margin (196). An aggressive surgical approach with adjuvant radiotherapy may enhance survival rates in patients with positive resection margins (197); conversely, there is no clear benefit of adjuvant radiotherapy in patients with negative resection margins (198).

1.5.2.5.2 Liver transplantation

For intrahepatic CCA patients, the initial experiments for liver transplantation are discouraging, with 5-year survival rates of up to only 18%, and therefore, this treatment usually is not recommended. Meyer *et al* have reported that more than 50% of 207 CCA patients undergoing liver transplantation experienced a recurrence within 2 years, with a median time from transplantation to recurrence of 9 months and a median time between recurrence and death of 2 months only (199). Preliminary results demonstrate that treatments with external-beam radiation, systemic fluorouracil (5FU), brachytherapy and liver transplantation are preferred therapies for early-stage patients. The same authors examined a neoadjuvant chemoradiation protocol that showed a 45% survival rate with a median follow-up time of 7 years (200,201). The greatest benefits from neoadjuvant radiochemotherapy and subsequent liver transplantation are possibly derived from patients under forty-five years of age that develop cholangiocarcinoma as a result of primary sclerosing cholangitis (202).

1.6 Rationale of this study

Among 810 individuals that died from liver cancer, ten to twenty percent perished from CCA (159,200). If detected at an early stage, CCA can be treated through surgical resection or liver transplantation as potential therapeutic options (165). However, most patients are diagnosed at an advanced stage of CCA, which explains the fact that CCA is a highly infiltrative tumor that expands and metastasizes within the liver. Epidemiologically, the incidence of CCA is variable due to differences in regional and environmental risk factors, such as chronic inflammation, fibropolycystic malformation, liver flukes, hepatitis B virus and hepatitis C virus infections (159,200).

Recent studies of other solid tumors have investigated the role and incidence of somatic mitochondrial mutations and their implications for carcinogenesis (117). Not only are mitochondria considered the powerhouses of the cell, but they also play an essential role in apoptosis; thus, it is important to understand the molecular aspects of mitochondrial DNA and their contribution to carcinogenesis. Moreover, mitochondrial DNA mutations have been demonstrated in multiple types of human cancers, including hepatocellular carcinoma, breast cancer, ovarian cancer and gastric cancer (117).

To the best of our knowledge, CCA etiology remains obscure; however, extensive studies of mtDNA mutations in CCA cell lines may shed a light on CCA pathogenesis for the purpose of investigating new therapeutic options.

1.7 Hypothesis and Thesis Objectives

This thesis tested the hypothesis that the mitochondria and their genome (mtDNA) alterations are common in human CCA.

The following objectives provided a systematic approach to test the hypothesis:

1) To scan mitochondrial DNA (mtDNA) including coding and non-coding regions and quantify the total mtDNA levels in CCA cell lines compared with normal hepatocytes, which further addresses of two specific aims:
   i) To detect homoplasmic and heteroplasmic alterations of mtDNA (see section 3.1);
   ii) To determine the copy number of mtDNA levels (see section 3.2).
2) To determine the morphological alterations of mitochondria that could be correlated with perturbations of mitochondrial functions in the CCA cell lines compared with normal hepatocytes, which consists three specific aims:
   i) To identify oxidative phosphorylation (OXPHOS) for protein content (see section 3.3);
   ii) To investigate ultrastructurally the cristae alterations (see section 3.4);
   iii) To measure the mitochondrial membrane potential $\Delta\Psi_m$ and to assess the mitochondrial metabolic alterations including L-Lactate and NAD^+/NADH (see sections 3.5 and 3.6).

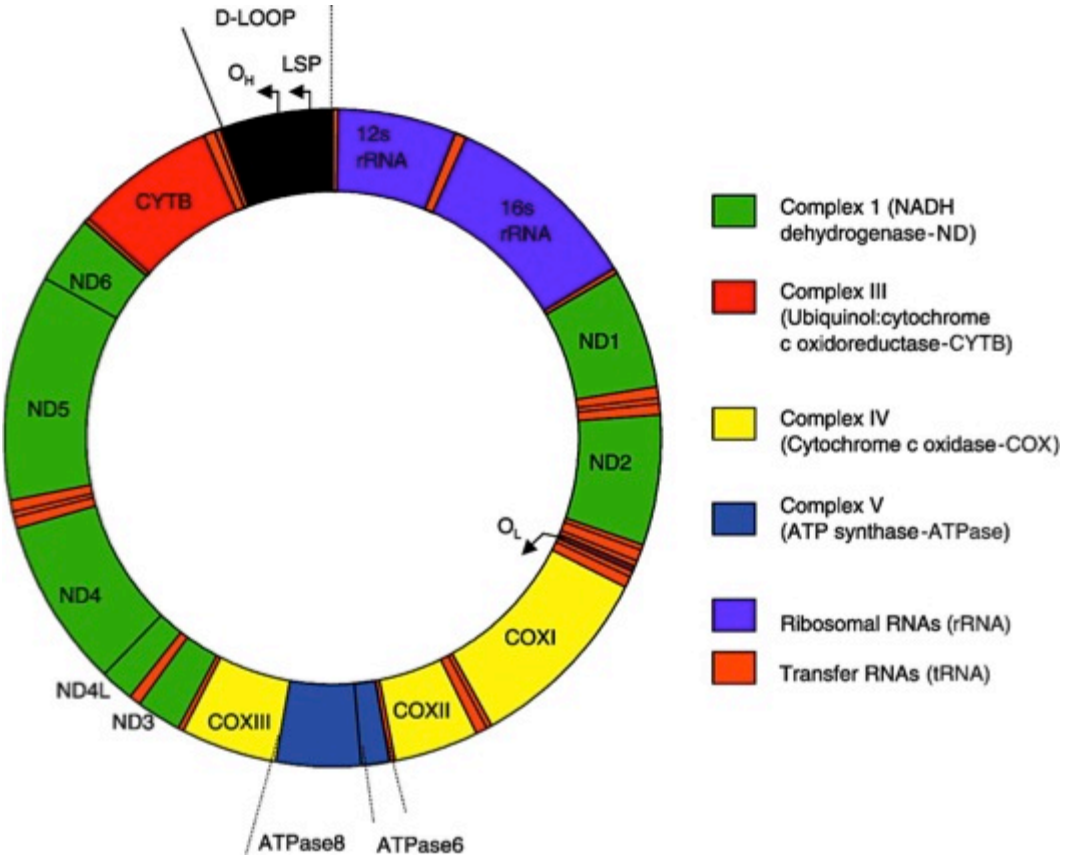

Figure 1.1 Mitochondrial genome structure (203)

Mammalian mtDNA is a double stranded molecule; composed of a H (heavy) strand and a L (light) strand and is approximately 16.5 kb in size. The origin for H-strand replication (OH) and the HSP and LSP transcription promoters are located in the D-loop (displacement loop). The origin for L-strand replication (OL) is located two thirds away around the genome from the D-loop. MtDNA encodes thirteen proteins of the electron transport chain (ETC). Twelve genes are located on the H-strand and only one gene is located on the L-strand. mtDNA also has 22 tRNAs and 2 rRNAs involved in mtDNA transcript production and processing.

Note: This figure was reproduced with permission from the publisher.

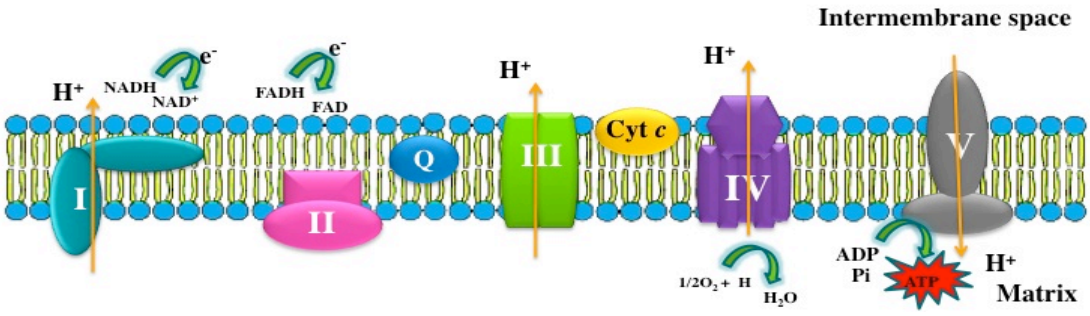

Figure 1.2 Oxidative phosphorylation: electron transport and ATP synthesis

The respiratory chain consists of four enzyme complexes (complexes I - IV) and two intermediary substrates (coenzyme Q and cytochrome c). Electrons are donated from NADH to NADH dehydrogenase, a large protein complex that pumps protons across the inner membrane. Then, electrons are transported to the cytochrome b-c complex via mobile molecule coenzyme Q (Q); the cytochrome b-c complex also pumps protons across the inner membrane. These electrons are delivered to the last protein complex, cytochrome oxidase, by the mobile protein cytochrome c (cyt c). Cytochrome oxidase donates the electrons to oxygen, and water is formed. Cytochrome oxidase also pumps protons across the membrane. The hydrogen concentration is much greater in the intermembrane space than in the matrix, thus generating an electrochemical proton gradient. This gradient drives protons back across the inner membrane through the ATP synthase that catalyzes the synthesis of ATP from ADP and inorganic phosphate (Pi).

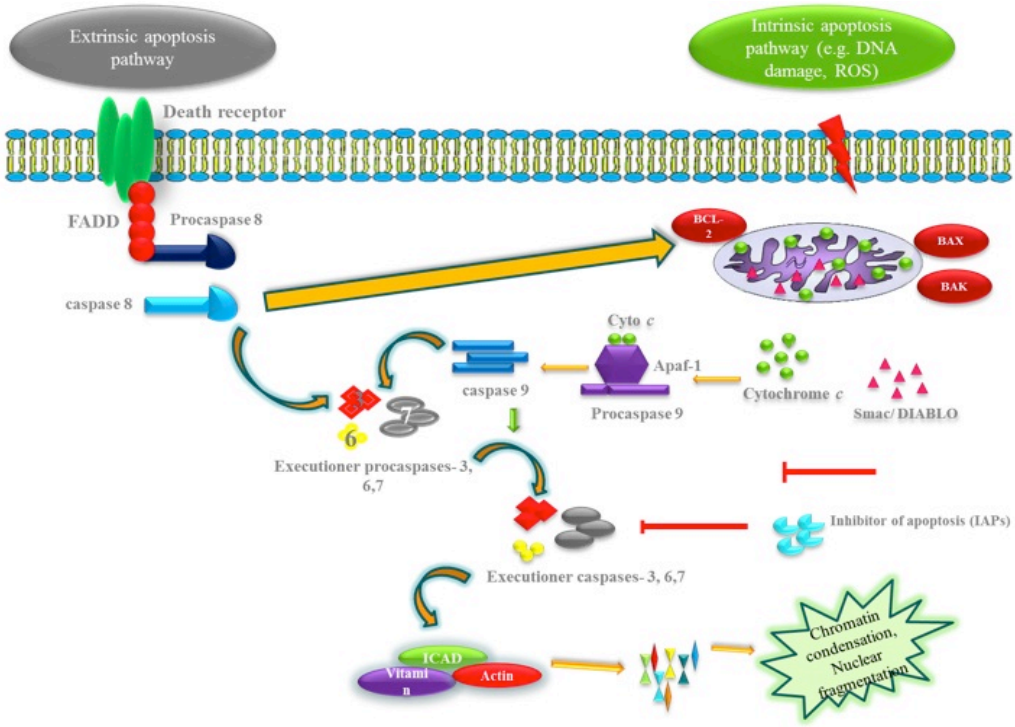

Figure 1.3 Apoptosis pathways

Apoptosis pathways can be initiated via different stimuli—that is, at the mitochondria (intrinsic pathway) or at the plasma membrane by death receptor ligation (extrinsic pathway). Mitochondria are engaged via the intrinsic pathway, which can be initiated by a variety of stress stimuli, including ultraviolet (UV) radiation, DNA damage and most chemotherapeutic agents. Mitochondrial membrane permeabilization is regulated by balance of opposing actions of proapoptotic and antiapoptotic Bcl2 family members (Bax, Bak, Bcl2 and Bcl-XL, Mcl-1). Following mitochondrial permeabilization, mitochondrial pro-apoptotic proteins like cytochrome c, Smac/Diablo release via transmembrane channels across the mitochondrial outer membrane (see main text for more details). Stimulation of death receptors results in receptor aggregation and recruitment of the adaptor molecule Fas-associated protein with death domain (FADD) and caspase-8. Upon recruitment, caspase-8 becomes activated and initiates apoptosis by direct cleavage of downstream effector caspases.

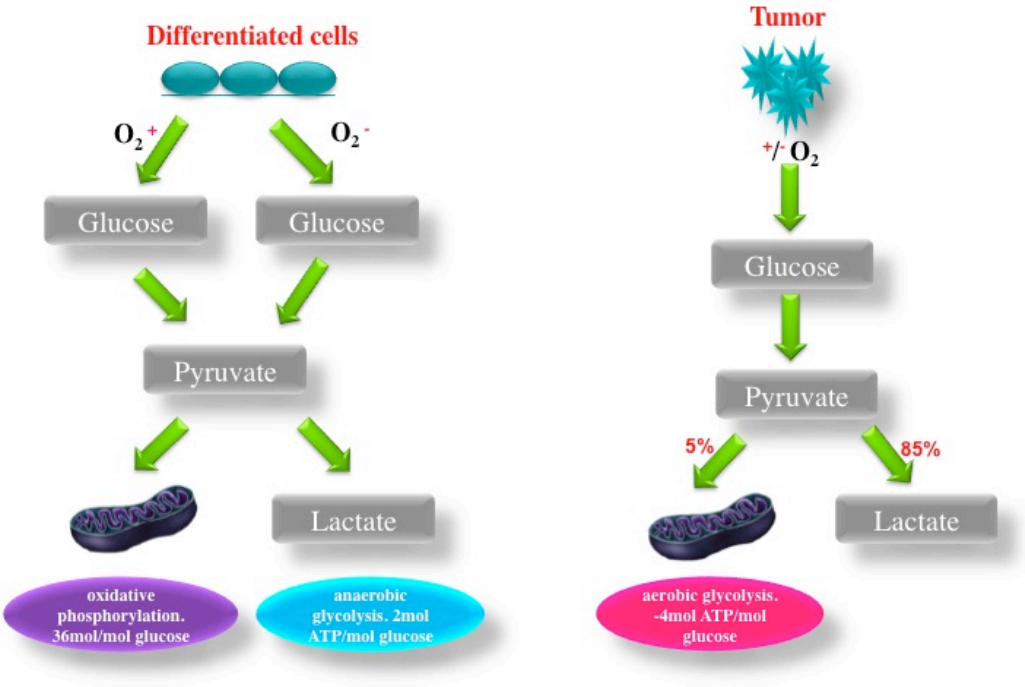

Figure 1.4 Warburg effect (204)

In the presence of oxygen, differentiated tissues first metabolize glucose to pyruvate via glycolysis and then completely oxidize most of that pyruvate in the mitochondria to CO2 during the process of oxidative phosphorylation. When oxygen is limiting, cells can redirect the pyruvate generated by glycolysis away from mitochondrial oxidative phosphorylation by generating lactate (anaerobic glycolysis). This generation of lactate during anaerobic glycolysis allows glycolysis to continue (by cycling NADH back to NAD+), but results in minimal ATP production when compared with oxidative phosphorylation. Warburg observed that cancer cells tend to convert most glucose to lactate regardless of whether oxygen is present (aerobic glycolysis).

Note: This figure was reproduced with permission from the publisher.

Chapter 2 Materials and Methods

2.1 Cell lines

Cholangiocarcinoma cell lines, HuCCT1 HuH28 and OZ were obtained from cell culture bank of the Japan Health Sciences Foundation and have been previously published in the literature (205,206). These cell lines were grown as a monolayer culture in their appropriate media. Briefly, HuCCT1 and HUH28 (moderately invasive cell lines) were cultured in RPMI 1680 medium, Roswell Park Memorial Institute, (Invitrogen Canada Inc. Burlington, ON, Canada) supplemented with 10% Fetal Bovine Serum (FBS, PAA laboratories Inc. Etobicoke, ON, Canada), 1ml gentamicin and incubated in a 5% CO_2 chamber at 37°C. OZ (metastasizing cell lines) was grown in William E medium (Invitrogen Canada Inc., Burlington, ON, Canada) supplemented with 10% FBS. We included the hepatocelluar carcinoma (HCC) cell lines to our investigational study (HepG2, Huh-7). Both cell lines were purchased from American Type Culture Collection (ATCC, Rockville, MD), cultured in DMEM medium, Dulbecco's Modified Eagle Medium, (Invitrogen Canada Inc., Burlington, ON, Canada) supplemented with 10% FBS, 1ml gentamicin and incubated in a 5 % CO_2 chamber at 37°C. An immortalized human liver cell line (THLE-3) was purchased from the American Type Culture Collection (ATCC, Rockville, MD). The cells were maintained in precoated flasks with a mixture of bronectin (0.01 mg/mL), bovine collagen type 1 (0.03 mg/ mL), and bovine serum albumin (0.01 mg/mL) dissolved in BEGM medium, bronchial tracheal epithelial cell growth medium, and incubated at 37°C and 5% CO2.

2.2 Human mitochondrial v2.0 oligonucleotide microarray

The MitoChip v2.0 was obtained from Affymetrix (commercially available GeneChip Human Mitochondrial Resequencing Array 2.0; Santa Clara, CA). Sequences comprising both strands of the entire human mitochondrial genome were synthesized as overlapping 25 bp oligonucleotides probe of defined sequence. To query any given site from human mitochondrial reference sequence, four features (A, C, G and T) are tiled on the MitoChip. The four features differ only by the 13th base, which consists of each of the four possible nucleotides.

2.2.1 MitoChip preparation

The total DNA was extracted from cell lines by using the QIAamp DNA Mini kit, which provides silica-membrane-based nucleic acid purification from cells, followed manufacturer's instructions (Qiagen, Inc., Valencia, CA). The final DNA was dissolved in doubly distilled water and frozen at -20 °C until use. Three pairs of overlapping primers were used to amplify the entire 16.6-kb mitochondrial genome. The three primer sets were F1: 5′-ATA GGG GTC CCT TGA CCA CCA TCC TCC GT-3′ and R1: 5′-GAG CTG TGC CTA GGA CTC CAG CTC ATG CGC CG-3′, F2: 5′-CCG ACC GTT GAC TAT TCT CTA CAA ACC AC-3′ and R2: 5′- GAT CAG GAG AAC GTG GTT ACT AGC ACA GAG AG- 3′, F3: 5′-CAT TCT CAT AAT CGC CCA CGG GCT TAC ATC C-3′ and R3: 5′-GTT CGC CTG TAA TAT TGA ACG TAG GTG CC-3′. Briefly, long-range PCR was performed using three PCR primer sets that can amplify the entire

mtDNA, using 100 ng of input DNA for each reaction of DNA template, 5U LA Taq polymerase (TaKara, Mississauga, ON, CA), 5 µL buffer, 2.5 mM each of dNTPs, 0.2 µM of primers were mixed with dH_20 to a final reaction volume of 50 µL. The cycling conditions for all reactions were: (1) 95°C for 2 min; (2) 95°C for 15 sec; (3) 68°C for 7 min; (4) repeat step 2 for 29 times; (5) final extension 72° for 12 min. As a control for PCR amplification and subsequent hybridization, a 7.5 kb plasmid DNA (Tag IQ-EX template) was amplified concomitantly with the test samples, using forward and reverse primers included in the CustomSeq™ kit (Affymetrix; Santa, CA). The PCR product was purified by using QIAQuick PCR Clean up kit (Qiagen, Inc., Valencia, CA). Spectrophotometric analysis was used to determine the concentration (ng/ µL) of the purified PCR product by measuring the absorbance at 260 nm (NanoDrop 1000 Spectrophotometer, Thermo Scientific, Wilmington, USA). The pooled 35 µl of DNA fragments were then digested with DNase I (0.2 U of DNase I/µg DNA) for 15 minutes in a 50-µl reaction (Affymetrix, Cat. 900447). Samples were then incubated at 95°C for 15 minutes to inactivate DNase I. Fragmented DNA was labeled by adding 2.0 µl of GeneChip DNA labeling reagent and 3.4 µl of 30 U/µl terminal deoxynucleotidyl transferase (both from Affymetrix; Santa, CA). The labeling conditions were 37°C 90 min and 95°C 15 min. Prehybridization, hybridization, washing, and scanning of the MitoChip were performed as described in the Affymetrix CustomSeq Resequencing protocol. Hybridization, washing and scanning were performed in array core laboratory at Benaroya Research Institute as described in Affymetrix CustomSeq Resequencing protocol (207).

2.2.2 Automated batch analysis of microarray data

Analysis of microarray data for the v2.0 MitoChip was done using GeneChip® Sequence Analysis Software (GSEQ) v 4.0 (Affymetrix; Santa, CA). GSEQ uses an objective statistical framework, based upon the ABACUS algorithm (126) to assign base calls to each position, which meets quality criteria in the mitochondrial genome. GSEQ assigned a base call at any position by using International Union of Pure and Applied Chemistry codes (IUPAC) afterward compared the base calls to the Cambridge reference sequence (rCRS). The base calls assigned either as a homoplasmic variant (mtDNA copies either wild-type or mutant in the same individual), heteroplasmic sequence variant (the mutant and wild-type of mtDNA copies coexist in the same individual), or N-call (207). Base changes not recorded in MitoMap (www.mitomap.org/MITOMAP) database were categorized as novel mtDNA variations in the database were categorized as reported mutation. GSEQ software was used per manufacturer's instructions (207), with Genome model set to "diploid" and Quality Score Threshold set to "3" to maximize base call percentage and fidelity.

2.3 Determination of MtDNA copy number

Mitochondrial DNA copy number was measured by a real-time PCR that uses the mitochondrial *ND1* gene as a marker of the entire mtDNA genome and normalized by simultaneous measurement of nuclear DNA encoded β- *actin* gene. DNA was harvested from confluent cultures of HuCCT1, HuH28, OZ, HepG2, Huh-7 and THLE-3 cells using the DNeasy tissue kit, which provides fast and easy silica-based DNA purification in convenient spin-column, followed

manufacturer's instructions (Qiagen, Inc., Valencia, CA). The DNA was quantified by spectrophotometry. The DNA abundance was measured using the TaqMan Universal PCR Master Mix with gene-specific MGB probe labeled with FAM and VIC fluorescent dyes (Applied Biosystems, Burlington, ON, Canada) using the StepOnePlus-Real time PCR System (Applied Biosystems, Burlington, ON, Canada). The sequences of the primers are: *β-actin* L-strand primer: 5′-CATGTGCAAGGCCGGCTTCG-3′, *β-actin* H-strand primer: 5′-CTGGGTCATCTTCTCGCGGT-3′, *ND1* L-strand primer: 5′-TCTCACCATCGCTCTTCTAC-3′, and *ND1* H-strand primer: 5′-TTGGTCTCTGCTAGTGTGGA-3′. Real-time PCR amplification was performed in 20 µl containing 2X TaqMan® Universal PCR Master Mix, No AmpErase® UNG, 1 μl 20X VIC®-RNase P Assay, 1 μl 20X FAM^{TM}-labeled gene specific assay, 8 μl DNase-free water, 200 nM each primer and 1 µl of each analyzed DNA sample. The concentration of each analyzed DNA sample was always 50 ng/µl. The PCR reactions (20 µL) was carried out in triplicate and the thermal cycling conditions were as follows: 95°C for 20sec followed by 40 cycles of 95°C for 1 sec and 60°C for 20sec. Threshold Cycle (CT) values for each time point were calculated by subtracting the CT of the endogenous gene from the CT of the target gene. Relative quantification values were determined using the $2^{-\Delta\Delta CT}$ methods and expressed as fold change in control (THLE-3) versus other cell lines. The content of *ND1* gene was normalized with the content of *β-actin* gene (nDNA) to calculate the relative mtDNA copy number in each sample.

2.4 Western blotting

The cultured cells were scraped in PBS and centrifuged at 670× *g* for 5 min. Cell pellets were lysed in 1× RIPA (radioimmunoprecipitation assay) buffer [25 mM Tris·HCl (pH 7.6), 150 mM NaCl, 1% Nonidet P-40, 1% sodium deoxycholate, and 0.1% SDS] supplemented with 1x protease inhibitor. Total protein was quantitated using the BCA (bicinchoninic acid) protein assay (Pierce, Thermo Scientific, ON, Canada). Western blot analysis was performed by using standard techniques. Fifty μg of protein was separated on gradient 4–20% SDS PAGE gels (Bio-Rad, Hercules, CA) and transferred into polyvinylidene fluoride (PVDF) membranes. Membranes then were incubated in tris-buffered saline (TTBS) supplemented with 5% non-fat dry milk for 3 hr at room temperature. Membranes were probed overnight with the OXPHOS cocktail of antibodies (1:200 dilutions, Mitoscience, Cambridge, Massachusetts, USA) targets the following proteins: 20-kD subunit of Complex I (20 kD), COX II of Complex IV (22 kD), 30-kD subunit of Complex II (30 kD), core 2 of complex III (~50 kD), and F1α (ATP synthase) of Complex V (~60 kD). Antibodies were then each probed with their corresponding HRP-conjugated secondary antibody (1:3,000 dilutions, Vector Laboratories, Burlingame, CA) for 1 hr at room temperature. The blots were visualized by using ECL Western blotting detection reagents (Amersham Biosciences, Piscataway, NJ) and developed on Kodak film (Kodak Graphic Communications Company, Burnaby, BC, Canada).

2.5 Electron microscopy

Briefly, confluent petri-dishes plates of each CCA and HCC cell lines were washed in PBS and fixed with 2% glutaraldehyde for 1 hr in 4°C. Cells were scrapped off form plates and collected in eppendorf tubes. After centrifugation, cell pellets were further fixed with osmium tetroxide overnight at room temperature. Afterward, following graded dehydration, pellets were epon-embedded and ultra-thin sectioned. Sections were mounted on metal mesh grids, and contrasted with uranyl acetate and lead citrate. Grids were examined in Hitachi H-7650 transmission electron microscope (TEM) (Hitach High-technologies Canada Inc. 89 Galaxy Blvd. Suite 14, Rexdale, ON M9W 6A4 Canada).

2.6 Measurement of mitochondrial membrane potential Δψm

The mitochondrial membrane potential sensor JC-1 (5,5′, 6,6′-Tetrachloro-1,1′,3,3′-tetraethyl-imidacarbocyanine iodide; Molecular Probes, Invitrogen, Germany) was used to label mitochondria in transmembrane manner. The JC-1 stock solution (5 mg/ml) was prepared in anhydrous dimethyl sulphoxide (DSMO) and diluted in supplemented culture medium with final concentration of 5 μg/ml. In physiologically polarized cells JC-1 accumulates at mitochondria as red fluorescent J-aggregates while in depolarized cells the dye forms green fluorescent monomers. The labeling procedure was applied following the heat treatments according to the manufacturer's recommendations. A confocal microscopy assay was performed with laser scanning confocal microscopy (Zeiss LSM 510) connected to an inverted microscope with a X40 water- immersion

objective lens, optimal laser lines and filter. The fluorescence of TMRE was excited at 564 nm and emitted signals were collected through 600 nm long pass filter. Images were digitized at 8 bits and analyzed using ZEN 2009 software (Carl Zeiss, Canada).

2.7 Lactate measurements

Lactate release was measured using a lactate assay kit from Eton Bioscience, Inc, San Diego, USA (cat no.1200012002). Briefly, two days before the experiment, cells were seeded in 10 cm dishes. At the time of measurement, cell density was about 60–70% confluent. Media from the dishes were collected and diluted to 50-fold with double-distilled water. Standard graph was generated using different concentrations of lactate in 50 µl of volume and 50 µl of lactate assay solution in 96-well plates followed by incubation in a humidified chamber at 37°C for 30 min. Similarly, different dilutions of media (2, 4, 6, 8, 10 µl/ml) were used to measure extracellular lactate in the linear range. Reaction was stopped by adding 50 µl of 0.5 M acetic acid and absorbance was measured at 490 nm using Synergy HT Microplate Reader.

2.8 NAD^+/NADH ratio assay

Cells were grown to 70% confluency in a 10 cm^2 tissue culture plate in appropriate media (as described above). NADH and NAD^+ were determined according to manufacturer's protocol (E2ND-100, Bioassay Systems, Hayward, CA). Briefly, cells were counted by trypan blue exclusion method, which

determine the number of viable cells present in a cell suspension. Cell pellets were resuspended in 1.5 mL Eppendorf tubes with either 100 µl NAD^+ extraction buffer (containing 0.40% hydrochloric acid) for NAD^+ determination or 100 µl NADH extraction buffer (containing 0.40% sodium hydroxide) for NADH determination. Extracts were heated for five min at 60°C and 20 µl of assay buffer (containing 3.0% Tris hydroxymethyl aminomethane and 0.10%BSA) was added followed by the extraction buffer to neutralise the extracts. Mixtures were vortexed and centrifuged at 13,000 rpm for five min. Supernatants were added to working reagent containing 60 µl assay buffer, 1 µl alcohol dehydrogenase, 1 µl ethanol, 14 µl phenazine methosulfate (PMS) and 14 µl tetrazolium dye (MTT). Optical density at 565 nm was recorded at time zero and at 15 min using a 96-well plate reader spectrophotometer (XMark, Bio-Rad, Mississauga, ON, Canada). Difference in absorbance was compared with standard solutions and used to calculate NADH and NAD^+ concentrations.

2.9 Statistical analysis

Data are expressed as mean±SEM, and the number of cells or experiments is shown as n. Statistical comparisons were made with the use of Student ***t*** test. All statistical results were calculated with SPSS 16.0 software and a P value <0.05 was regarded as significant.

Chapter 3 Results

3.1 Mitochip analysis

To define the pattern and frequency of mtDNA mutations in CCA, a total of 226,536 mtDNA bases of were sequenced in the three cell lines with a median call rate of 97.9% (Table 3.1). Consequently, all three cell lines demonstrated at least 24 mtDNA alterations. Of the 102 mtDNA alterations observed in the three CCA cell lines, 38 of these alterations were synonymous and 30 of them were involved in non-coding, including ribosomal and transfer RNA (Table 3.2). Twenty-eight alterations were non-synonymous coding region mutations, resulting in an amino acid change. Of the 51 alterations observed in Papova-immortalized normal hepatocyte cell lines (THLE-3), 11 were non-synonymous coding region alterations (Table 3.3), 22 were synonymous variations and 17 alterations were involved in non-coding, including ribosomal and transfer RNA (Table 3.2). Among these alterations, three heteroplasmic mutations in each of HuCCT1 and Huh-28 were found to be novel. One of these unique alterations was present in Huh-28; specifically, this (T16315G) alteration was located in the control region of mtDNA, which contains silent variations with no amino acid changes. The remaining novel alterations were located in protein coding regions, three of which were present in the *ND3* gene, one of which was located in *ATPase6* and one was existed in *COI*. All of these alterations caused amino acid changes in highly conserved residues (Table 3.4). Overall, the mtDNA alterations most commonly present in all cell lines, which were moderately invasive and metastasizing lines, involved the *D-loop, 12S rRNA, 16S rRNA, ND2, ND4, ND5,*

COI, ATPase6 and *CYTB* genes (Figure 3.1). Additionally, we identified two regions of the mitochondrial genome, the *D-loop* and *CYTB,* which are selectively mutated at a higher rate than other genes. Surprisingly, the metastasizing cell line, OZ, displays no mutation in the genes *ND1, ND3, ND6, CII* and *CIII*, which are mainly present in Complex I and Complex IV. However, OZ is the only cell line that contains a mutation in *ND4L* (Table 3.2).

Among the 76 mtDNA alterations observed in the two HCC cell lines, HepG-2 and HuH-7, 19 alterations were non-synonymous coding region mutations, thus resulting in an amino acid change. Additionally, 27 alterations were synonymous and 20 variations were involved in non-coding, including ribosomal and transfer RNA (Table 3.2). The most common mutations present in both cell lines were involved in the following genes: *D-loop, 12S rRNA, 16S rRNA, ND1, ND2, ND4, ND5, COI, COIII, ATPase6* and *CYTB*. Among these variations, ten alterations were identified as novel in HCC cell lines, six of which occurred in Huh-7 and four were present in HepG-2. All of these unique alterations were heteroplasmic with the exception of two homoplasmic modification, which were present in Huh-7 G15002A *CYB* and T13277C *ND5* genes. The novel heteroplasmic alterations were found in protein coding regions; however, two alterations were present in the *12SRNA* gene in HuH-7 and the control region, or *D-loop*, in HepG-2 (Table 3.4). Nevertheless, some alterations are only present in HuH-7 cell lines, including *ND3* and *COII* (Figure 3.2*),* while the *ND6* mutation is only present in HuH-28, which is absent in both HCC cell lines.

Several recurrent sequence alterations were observed in all CAA, HCC and immortalized hepatocyte cell lines (Table 3.2). Notably, all of these alterations were homoplasmic and present in *COI, ATPase6, ND4, ND5, and CYB*; however, the significance of these recurrent alterations in the carcinogenesis and the progression in CCA and HCC remains unclear.

3.2 Alterations in mtDNA copy number of CCA and HCC cell lines versus normal hepatocyte cell line

To investigate mtDNA copy number changes occurred in CCA and HCC, we further analyzed mtDNA copy number in CCA and HCC cell lines compared with immortalized hepatocyte cell line by real-time PCR. All CCA (HuCCT1, HuH28, OZ) cell lines showed marked reduction of mtDNA copy number compared with immortalized hepatocyte cell line. The average of mtDNA copy number/β-actin level in CCA was significantly lower than that in immortalized hepatocyte cell line ($P<0.05$) ($P= .021$, $P= .017$, $P= .040$), respectively (Figure 3.3). The hepatocellular carcinoma cell lines HepG-2 and Huh-7 had less total mitochondrial DNA than immortalized hepatocyte cell line; however, the differences between HCC and immortalized hepatocyte cell line were not significant ($P= .437$, $P= .083$), respectively (Figure 3.3).

3.3 Analysis of OXPHOS proteins of CCA and HCC cell lines versus normal hepatocyte cell line

Respiratory protein content, OXPHOS, was reduced in CCA and HCC. Moreover, immunoblot analyses indicated that the cellular content of the nuclear

and mitochondrial encoded proteins; Complex I and Complex III were reduced in CCA and HCC cell lines when compared with immortalized hepatocyte cell line (Figure 3.4).

3.4 Morphology of mitochondria in CCA and HCC cell lines using electron microscopy versus normal hepatocyte cell line

As shown in Figure 3.5.a, HuCCT1 showed primitive mitochondria elements with an oval shape, some of which were remarkably absent of cristae. HuH-28 (Figure 3.5.b) exhibited a dense matrix with decreased cristea. OZ cell line has a normal matrix, with absent cristea in both ovular and tubular shaped mitochondria; in addition, dense bodies were found in some mitochondria as well as in cytosol. Interestingly, glycogen material or endoplasmic reticulum surrounded the mitochondria (Figure 3.5.c). Also, HepG2 (Figure 3.5.d) displayed ovular mitochondria with a dense matrix and aberrant cristae. Finally, HuH-7 (Figure 3.5.e) showed both tubular and ovular mitochondria, some of which possessed a decreased number of cristae; however, while there were focal abnormalities, there were no dense bodies. All CCA and HCC cell lines were compared with normal hepatocyte cell lines, THLE-3 (Figure 3.5.f), which revealed a decreased amount of cristae whose size and shape identified tubular mitochondria.

3.5 Mitochondrial membrane potential Δψm of CCA and HCC cell lines versus normal hepatocyte cell line

The intensity of the fluorescent TMRE (tetramethylrhodamine ethyl ester) probe was used as an indirect measure of mitochondrial inner membrane potential ($\Delta\Psi_m$) in CCA and HCC cell lines. Immunoflourescnce images showed that the normal cell line (Figure 3.6.f) was hyperpolarized compared to all CAA and HCC cell lines (Figure 3.6.a-e), which were depolarized. These results suggested that there were some changes of mitochondrial function in the cancer cell lines.

3.6 Determination of intracellular metabolite concentrations of CCA and HCC cell lines versus normal hepatocyte cell line

We measured Lactate and NAD^+/NADH ratio in both CCA and HCC cell lines. As a lactate is the product of anaerobic glycolysis, mitochondrial dysfunction is usually associated with hyperlactatemia in normal aerobic conditions (208). As shown in Figure 3.7, lactate measurements significantly increased in all CCA cells lines (P= .03, P= .05, P= .02), respectively, and in HuH-7 (P=.02) of HCC cell lines, indicating an increasing adaptation on glycolysis with increasing alterations of mtDNA. In addition, All CCA and HCC cell lines except HuH-28 showed significantly high NADH levels comparing to normal hepatocyte (Figure 3.8).

Table 3.1 Summary of array-based analysis for mtDNA alterations

Summary of analysis	
Number of sample analyzed	6
mtDNA bases per MitoChip v2.0 microarray	6,569
Total number of mtDNA bases sequenced	226,536
Total number of mtDNA bases assigned by genotyping software	163,348
Percent overall bases call rate	97%
Range of bases called across 6 arrays	95.6%-99.5%
Median base call rate	97.9%

Table 3.2 mtDNA alterations in cholangiocarcinoma (CCA) and hepatocellular carcinoma cell lines and immortalized hepatocyte cell lines.

Cell lines	NTD Pos	Gene location	RCRS	Alteration	Amino acid	Homoplasmy OR heteroplasmy
HUCCT1						
	4071	ND1	C	T	Y-Y	Homo
	4164	ND1	A	G	M-M	Homo
	4769	ND2	A	G	M-M	Homo
	5351	ND2	A	G	L-L	Homo
	6455	COI	C	T	F-F	Homo
	6680	COI	T	C	T-T	Homo
	7028	COI	C	T	A-A	Homo
	7684	COII	T	C	L-L	Homo
	9540	COIII	T	C	L-L	Homo
	9824	COIII	T	C	L-L	Homo
	10400	ND3	C	T	T-T	Homo
	10873	ND4	T	C	P-P	Homo
	11719	ND4	G	A	G-G	Homo
	12405	ND5	C	T	L-L	Homo
	12705	ND5	C	T	I-I	Homo
	14783	CYB	T	C	L-L	Homo
	15043	CYB	G	A	G-G	Homo
	15301	CYB	G	A	L-L	Homo
HUH28						
	4769	ND2	A	G	M-M	Homo
	7028	COI	C	T	A-A	Homo
	9242	COIII	A	G	K-K	Homo
	9540	COIII	T	C	L-L	Homo
	10400	ND3	C	T	T-T	Homo
	11719	ND4	G	A	G-G	Homo
	12705	ND5	C	T	I-I	Homo
	14308	ND6	T	C	G-G	Homo
	14783	CYB	T	C	L-L	Homo
	15301	CYB	G	A	L-L	Homo
OZ						
	4769	ND2	A	G	M-M	Homo
	5147	ND2	G	A	T-T	Homo
	5417	ND2	G	A	Q-Q	Homo
	7028	COI	C	T	A-A	Homo
	8841	ATPase6	C	T	A-A	Homo
	10607	ND4L	C	T	L-L	Homo

	11719	ND4	G	A	G-G	Homo
	12501	ND5	G	A	M-M	Homo
	12705	ND5	C	T	I-I	Homo
	14893	CYB	A	G	L-L	Homo
HUH7						
	4071	ND1	C	T	Y-Y	Homo
	4164	ND1	A	G	M-M	Homo
	4769	ND2	A	G	M-M	Homo
	5351	ND2	A	G	L-L	Homo
	6455	COI	C	T	F-F	Homo
	6680	COI	T	C	T-T	Homo
	7028	COI	C	T	A-A	Homo
	7684	COII	T	C	L-L	Homo
	9540	COIII	T	C	L-L	Homo
	10400	ND3	C	T	T-T	Homo
	11719	ND4	G	A	G-G	Homo
	12405	ND5	C	T	L-L	Homo
	12705	ND5	C	T	I-I	Homo
	14783	CYB	T	C	L-L	Homo
	15043	CYB	G	A	G-G	Homo
	15301	CYB	G	A	L-L	Homo
HEPG2						
	4755	ND2	T	C	L-L	Homo
	4769	ND2	A	G	M-M	Homo
	4820	ND2	G	A	E-E	Homo
	4976	ND2	A	C	G-G	Hetero
	4977	ND2	T	C	L-L	Homo
	6473	COI	C	T	I-I	Homo
	7028	COI	C	T	A-A	Homo
	7241	COI	A	G	A-A	Homo
	9950	COIII	T	C	V-V	Homo
	11719	ND4	G	A	G-G	Homo
	13590	ND5	G	A	L-L	Homo
THLE-3						
	3594	ND1	C	T	V-V	Homo
	4104	ND1	A	G	L-L	Homo
	4769	ND2	A	G	M-M	Homo
	7028	COI	C	T	A-A	Homo
	7175	COI	T	C	T-T	Homo
	7256	COI	C	T	N-N	Homo
	7274	COI	C	T	G-G	Homo

	7771	COII	A	G	E-E	Homo
	9221	COIII	A	G	S-S	Homo
	9540	COIII	T	C	L-L	Homo
	10115	ND3	T	C	I-I	Homo
	11719	ND4	G	A	G-G	Homo
	11914	ND4	G	A	T-T	Homo
	11944	ND4	T	C	L-L	Homo
	12693	ND5	A	G	K-K	Homo
	12705	ND5	C	T	I-I	Homo
	13590	ND5	G	A	L-L	Homo
	13650	ND5	C	T	P-P	Homo
	13803	ND5	A	G	T-T	Homo
	14566	ND6	A	G	G-G	Homo
	15301	CYB	G	A	L-L	Homo
	15784	CYB	T	C	P-P	Homo

RCRS= Revised Cambridge Reference Sequence; both the RCRS position and refrence nucleotide at that position are designed. Hetero mut=heteroplasmy mutation, homo mut= homoplasmy mutation
The MitoAnalyzer tool (http://www.cstl.nist.gov/biotech/strbase/mitoanalyzer-direction.html) was used for determining the effect of base substitution on translated protein sequence.
The bold base positions are recurrent alterations present in all CCA and HCC cell lines and normal hepatocyte cell line.

Table 3.3 Non-synonymous mitochondrial DNA and amino acid alterations in cholangiocarcinoma (CCA) and hepatocellular carcinoma (HCC) and immortalized hepatocyte cell lines.

Cell lines	NTD Pos	Gene location	RCRS	Alteration	Amino acid	Homoplasmy OR heteroplasmy
HUCCT1						
	3308	ND1	T	C	M-T	Homo
	4048	ND1	G	A	D-T	Homo
	5460	ND2	G	A	A-T	Homo
	7853	COII	G	A	V-I	Homo
	8701	ATPase6	A	G	M-V	Homo
	8860	ATPase6	A	G	T-A	Homo
	9539	COIII	A	C	Q-H	Homo
	10345	ND3	T	C	I-T	Homo
	10398	ND3	A	G	T-A	Homo
	12811	ND5	T	C	Y-H	Homo
	14766	CYB	C	T	T-I	Homo
	15326	CYB	A	G	T-A	Homo
	15756	CYB	G	A	W-TER	Hetero
HUH28						
	3394	ND1	T	C	Y-M	Homo
	3407	ND1	G	A	R-H	Hetero
	4491	ND2	G	A	L-I	Homo
	8701	ATPase6	A	G	T-A	Homo
	8860	ATPase6	A	G	T-A	Homo
	9243	COIII	C	G	P-A	Hetero
	10398	ND3	A	G	T-A	Homo
	11963	ND4	G	A	V-I	Homo
	14766	CYB	C	T	T-I	Homo
	15326	CYB	A	G	T-A	Homo
OZ	**8860**	ATPase6	A	G	T-A	Homo
	11016	ND4	G	A	S-N	Homo
	13183	ND5	A	G	I-V	Homo
	14766	CYB	C	T	T-I	Homo
	15326	CYB	A	G	T-A	Homo
HUH7						
	3392	ND1	G	A	G-D	Hetero
	4048	ND1	G	A	D-G	Homo
	5460	ND2	G	A	A-T	Homo
	8701	ATPase6	A	G	M-V	Homo

	8860	ATPase6	A	G	T-A	Homo
	9539	COIII	A	C	Q-H	Hetero
	10345	ND3	T	C	I-T	Homo
	10398	ND3	A	G	T-A	Homo
	12811	ND5	T	C	Y-H	Homo
	13276	ND5	A	M	M-L	Hetero
	14766	CYB	C	T	T-I	Homo
	15326	CYB	A	G	T-A	Homo
	15758	CYB	A	G	I-V	Homo
HEPG2						
	3547	ND1	A	G	I-V	Homo
	8860	ATPase6	A	G	T-A	Homo
	11177	ND4	C	T	P-S	Homo
	14757	CYB	T	C	M-T	Homo
	14766	CYB	C	T	T-I	Homo
	15326	CYB	A	G	T-A	Homo
THLE-3						
	7173	COI	A	C	T-A	Hetero
	7770	COII	A	G	E-G	Hetero
	8701	ATPase6	A	G	T-A	Homo
	8860	ATPase6	A	G	T-A	Homo
	9539	COIII	A	C	Q-H	Hetero
	10398	ND3	A	G	T-A	Homo
	11945	ND4	A	C	T-P	Hetero
	12694	ND5	T	G	Y-D	Hetero
	13805	ND5	C	G	A-G	Hetero
	14766	CYB	C	T	T-I	Homo
	15326		A	G	T-A	Homo

RCRS= Revised Cambridge Reference Sequence; both the RCRS position and refrence nucleotide at that position are designed. Hetero mut=heteroplasmy mutation, homo mut= homoplasmy mutation.
The MitoAnalyzer tool (http://www.cstl.nist.gov/biotech/strbase/mitoanalyzer-direction.html) was used for determining the effect of base substitution on translated protein sequence.
The bold base positions are recurrent alterations present in all CCA and HCC cell lines and normal hepatocyte cell line.

.

Table 3.4 Novel mtDNA alterations in cholangiocarcinoma (CCA) and hepatocellular carcinoma (HCC) and immortalized hepatocyte cell lines.

Cell lines	NTD Pos	Gene location	RCRS	Alteration	Amino acid	Homoplasmy OR heteroplasmy
HUCCT1						
	6678	COI	A	C	T-P	Hetero
	9179	ATPase6	T	C	V-A	Hetero
	10399	ND3	C	G	T-S	Hetero
HUH28						
	10399	ND3	C	G	T-S	Hetero
	10401	ND3	G	T	E-TER	Hetero
	16315	D-loop	T	G	NA	Hetero
HUH7						
	1285	12S rRNA	G	T	NA	Hetero
	6678	COI	A	C	T-P	Hetero
	9179	ATPase6	T	C	V-A	Hetero
	10399	ND3	C	G	T-S	Hetero
	13277	ND5	T	C	M-T	Homo
	15002	CYB	G	A	G-S	Homo
HEPG2						
	4759	ND2	T	C	M-T	Hetero
	14756	CYB	A	C	M-L	Hetero
	14772	CYB	C	T	P-L	Hetero
	16521	D-loop	A	C	NA	Hetero
THLE-3						
	2620	16S rRNA	G	A	NA	Hetero

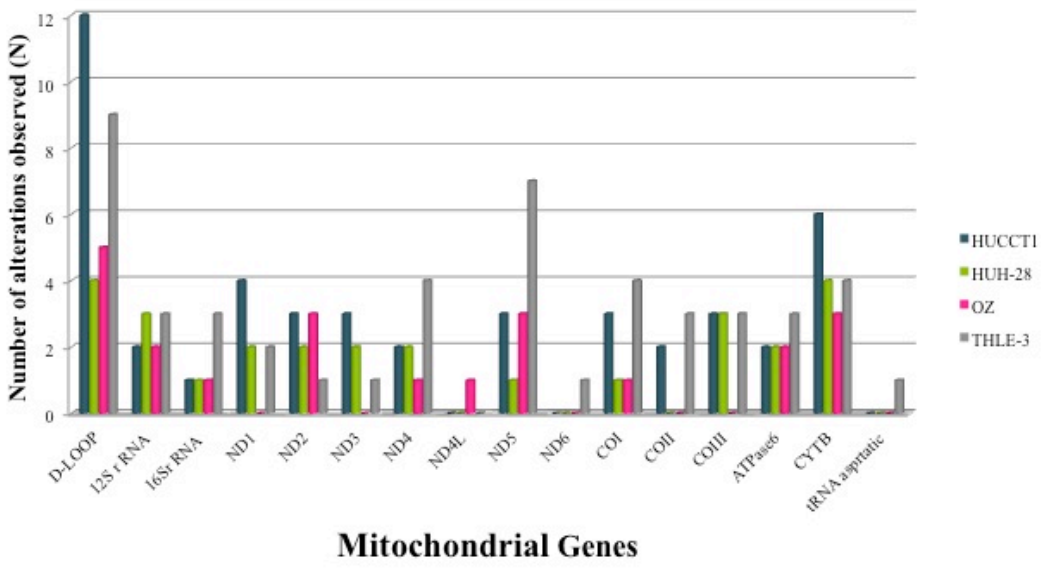

Figure 3.1. MitoChip analysis for CCA and immortalized hepatocyte cell lines

Of the 102 alterations observed in the 3 cell lines, 28 were non-synonymous coding region alterations (i.e., resulting in an amino acid change), 38 synonymous, 30 involved in non-coding including ribosomal, transfer RNA and D-loop and 6 were novel alterations. Of the 51 alterations observed in Papova- immortalized normal hepatocyte cell line (THLE-3), 11 were non-synonymous coding region alterations, 22were synonymous and 17 alterations were involved in non-coding, including ribosomal, transfer RNA and D-loop and one was novel alteration.

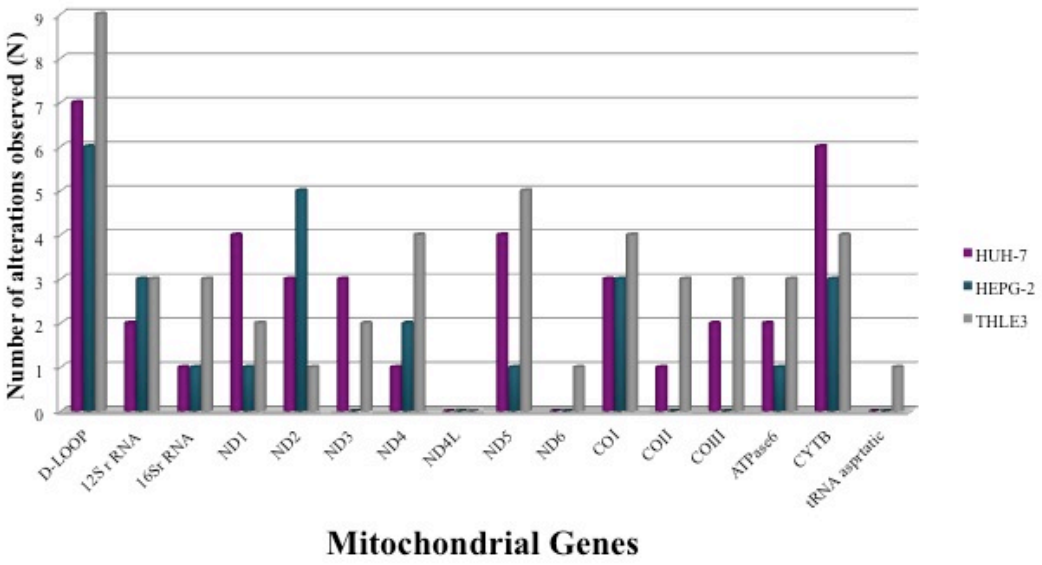

Figure 3.2. MitoChip analysis for HCC and immortalized hepatocyte cell lines

Of the 76 mutations observed in the 2 cell lines (HEPG-2, HuH-7), 19 were non-synonymous coding region mutations (i.e., resulting in an amino acid change), 27 synonymous and 20 involved in non-coding including ribosomal transfer RNA and D-loop and 10 were novel alterations. Of the 51 alterations observed in Papova- immortalized normal hepatocyte cell line (THLE-3), 11 were non-synonymous coding region alterations, 22were synonymous and 17 alterations were involved in non-coding, including ribosomal, transfer RNA and D-loop and one was novel alteration.

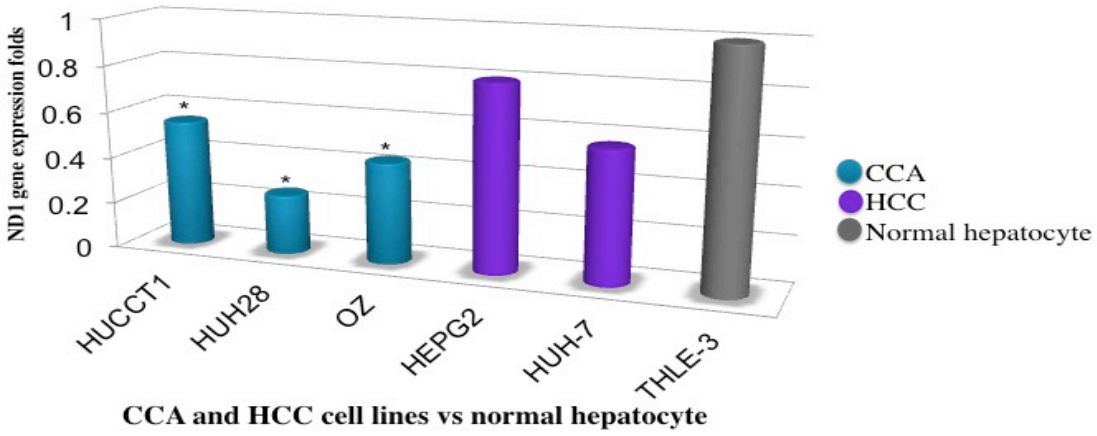

Figure 3.3 Mitochondrial DNA copy number for CAA, HCC and immortalized hepatocyte cell lines

Relative quantification values were determined by using the 2 -ΔΔCT method and expressed as fold change in control (THLE-3) versus other cell lines. Genes analyzed were β-actin (endogenous gene) and ND1 (gene of interest). $P \leq 0.05$ considered as significant.

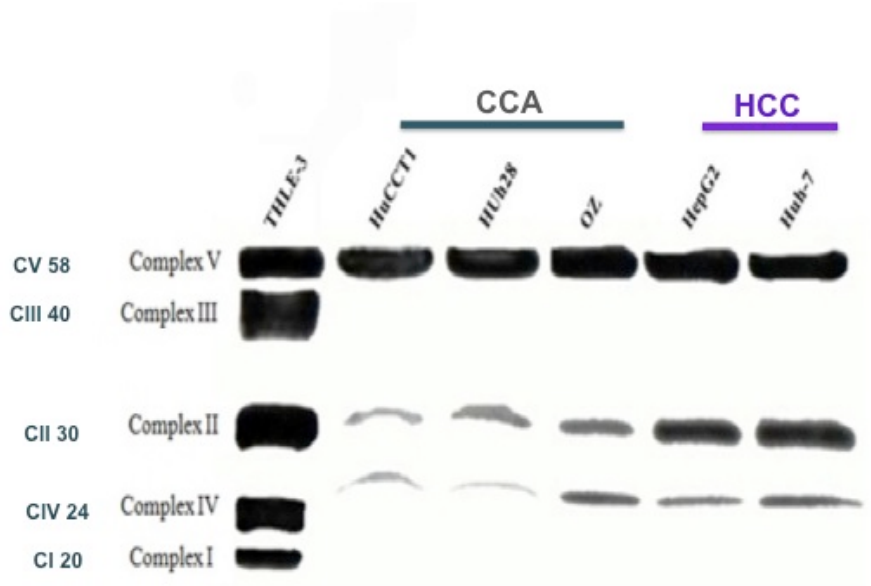

Figure 3.4 Analysis of OXPHOS proteins for CAA, HCC and immortalized hepatocyte cell lines

Mitochondrial respiratory proteins in cholangiocarcinoma & Hepatocellular carcinoma show decreased levels of the nuclear and mitochondrial encoded proteins, complex I and complex III.

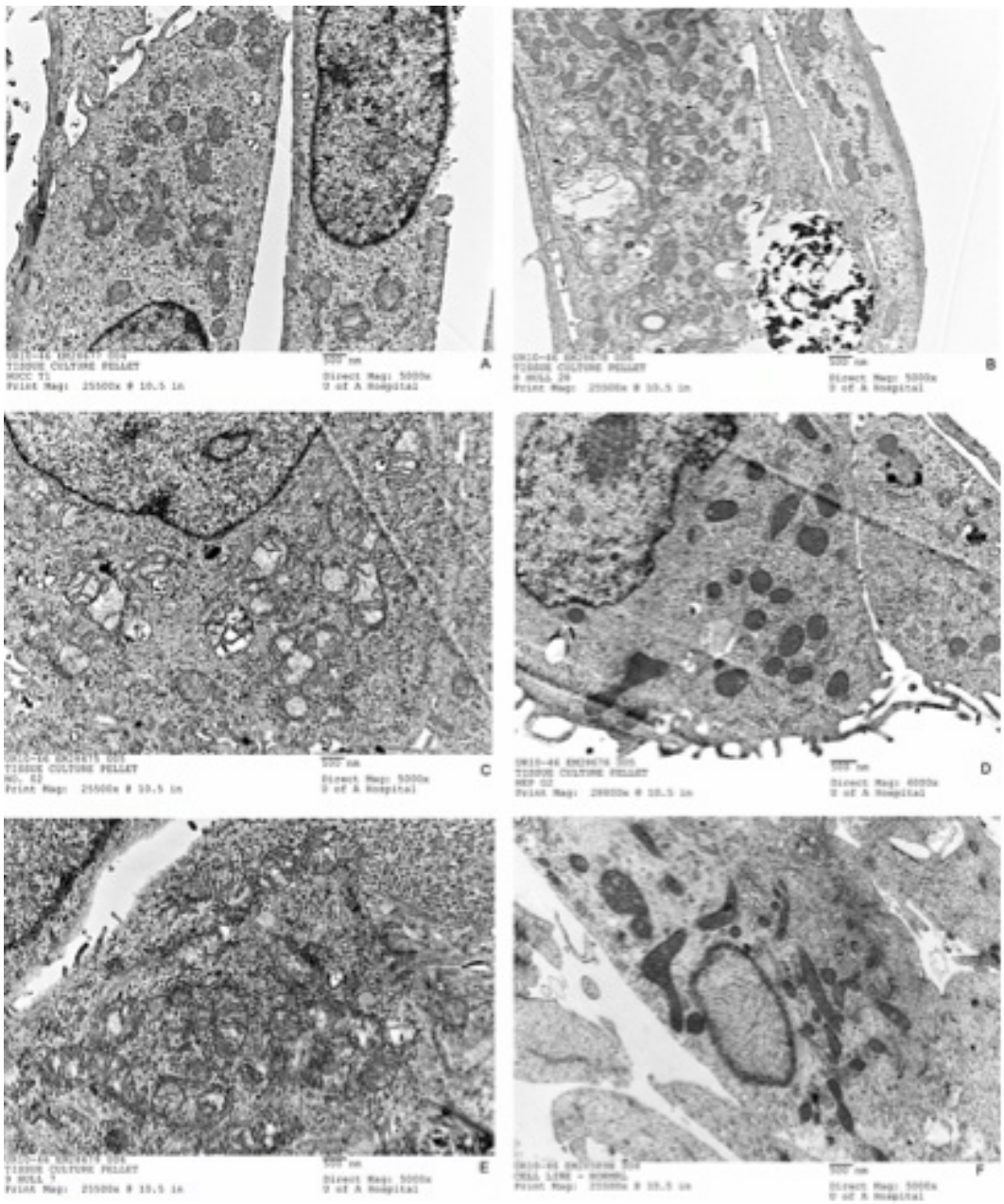

Figure 3.5 Electron microscopic images for ultrastructural and mitochondrial cristae alterations in CAA HuCCT1 (a), HuH28 (b), OZ(c), HCC (HepG2 (d), Huh-7 (e) and immortalized hepatocyte (THLE-3 (f) cell lines

.

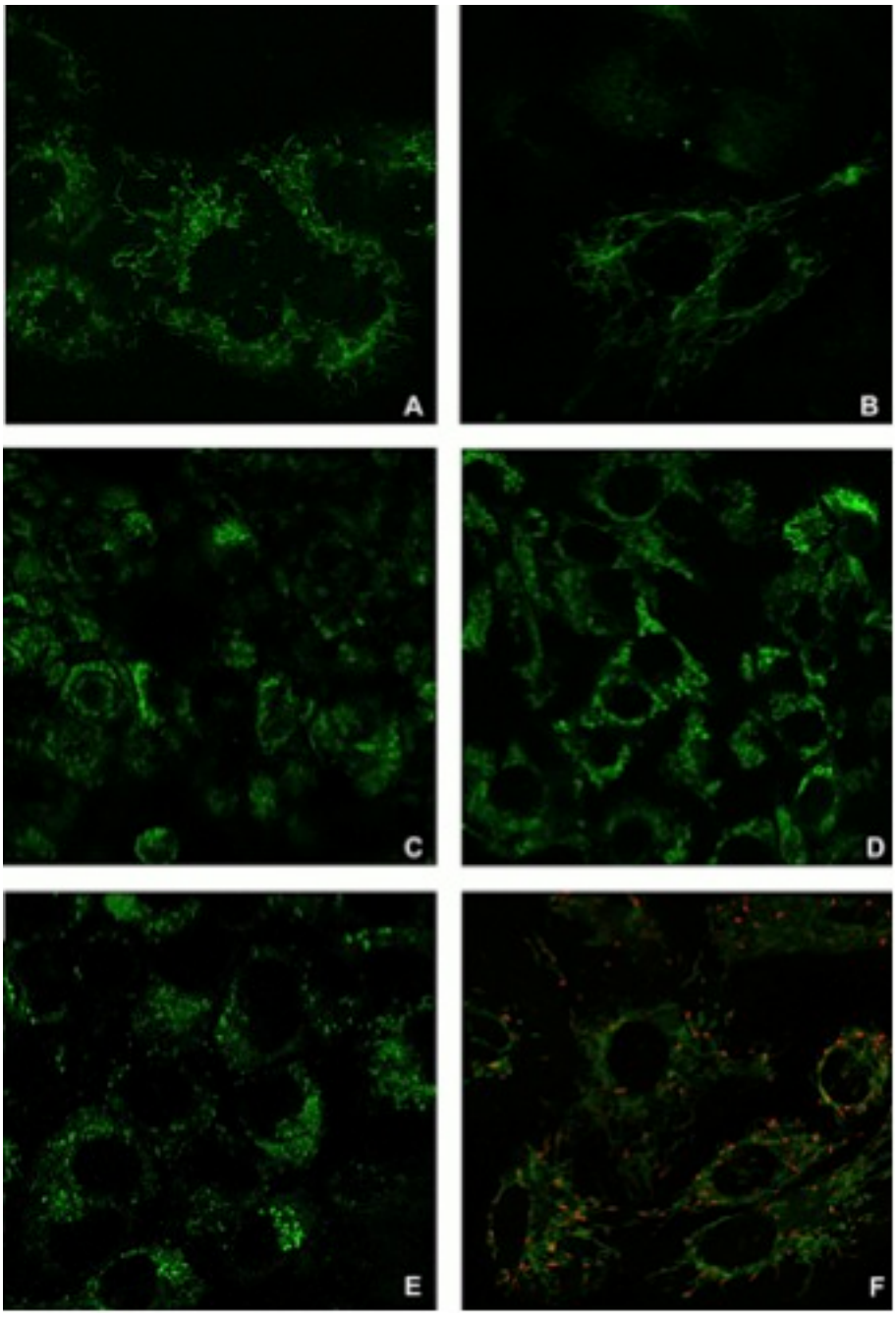

Figure 3.6 Confocal images of mitochondrial inner membrane potential ($\Delta\Psi_m$) CAA (HuCCT1 (a), HuH28 (b), OZ (c), HCC (HepG2 (d), Huh-7 (e) and immortalized hepatocyte THLE-3 (f) cell lines

Regions of high mitochondrial polarization are indicated by red fluorescence due to J-aggregate formation by the concentrated dye. Depolarized regions are indicated by the green fluorescence of the JC-1 monomers.

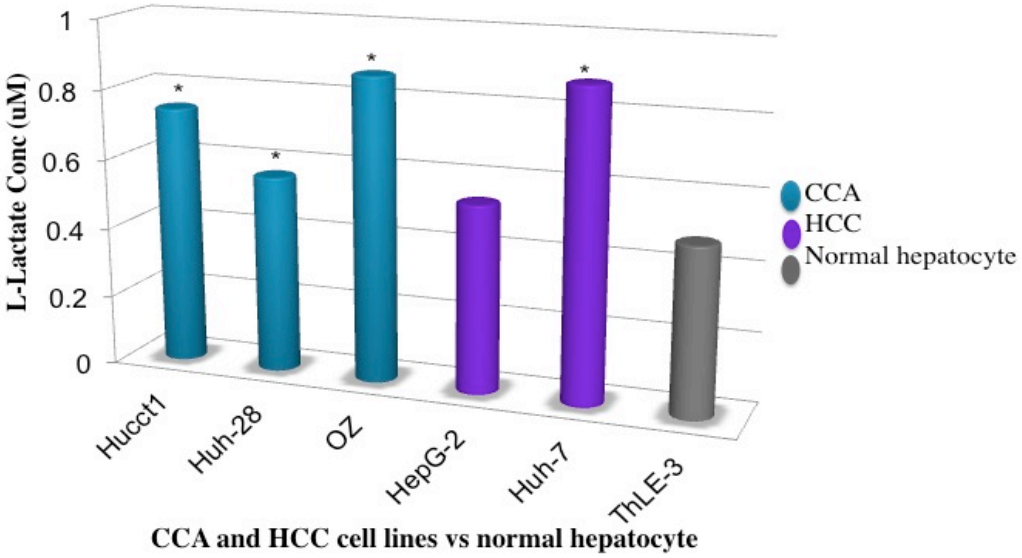

Figure 3.7 Extracellular lactate level for CAA, HCC and immortalized cell lines

It was determined in the media from 1×10^6 cells and calculated after 48 h of culturing. Lactate measurements significantly increased in all CCA cells lines and in HuH-7 of HCC cell lines. Data are mean±SD. Data were confirmed by 3 independent experiments. (*$P <$ 0.05) was regarded as significant.

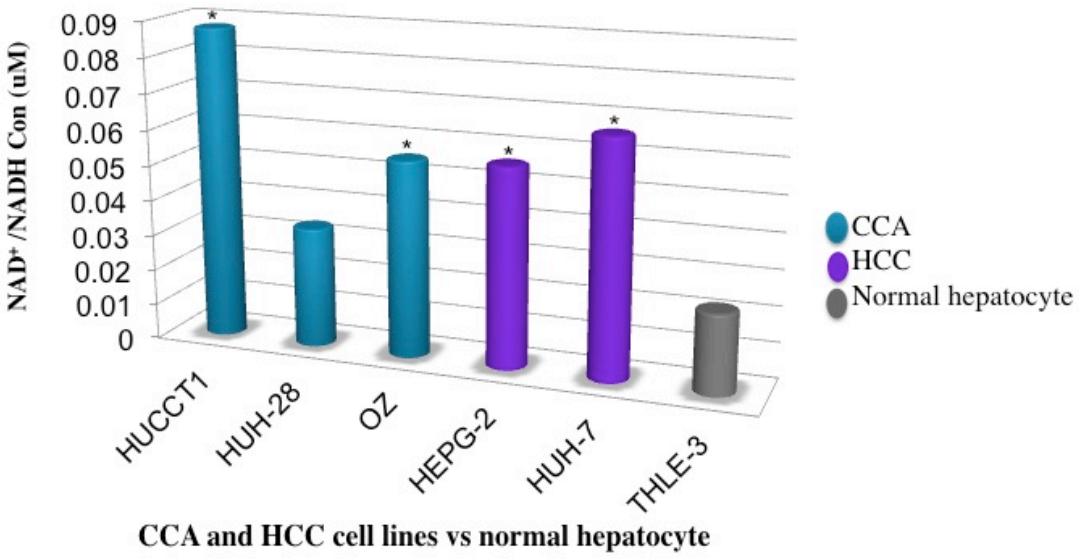

Figure 3.8 Cytosolic free NAD/NADH ratios in CCA, HCC and immortalized cell lines

All CCA and HCC cell lines except HuH-28 significantly showed high NADH levels comparing to normal hepatocyte. Data are mean±SD. Data were confirmed by 3 independent experiments. (*$P <$ 0.05) was regarded as significant.

Chapter 4 Discussion

4.1 General discussion

This study represents the first detailed investigation of the entire mitochondrial genome in cholangiocelluar carcinoma and hepatocellular carcinoma cell lines, which have been extensively studied on a large scale with human patient samples (209,210). Specifically, we screened the entire mitochondrial genome of three cholangiocelluar carcinoma and two hepatocellular carcinoma cell lines for the presence of mitochondrial alterations. In this process, we used the MitoChip array, comparing it with the revised Cambridge Reference Sequence (rCRS) to evaluate the nucleotide alterations. Since the corresponding non-cancerous cells were not available, which would differentiate mutations from rare polymorphisms, we relied on the MitoChip and the rCRS.

4.2. Mitochondrial control region base pair changes

Although alterations occurred along the entire mitochondrial genome, most of these changes were localized in the D-loop. The mitochondrial D-loop, approximately 1 kb in size, contains *cis*-acting elements involved in regulating the transcription and replication of the mitochondrial genome (11). We found that all of the cell lines with mtDNA alterations contained at least one of the D-loop, tRNA, rRNA or non-synonymous coding alterations (Figure 3.1 and 3.2); hence acquiring the potential for altering mitochondrial function via alterations in transcription, translation and replication. Our findings of asymmetric alterations in

the D-loop are consistent with previous studies showing modifications in the regulation of the mitochondrial genome, which may be associated with carcinogenesis in CCA and HCC (211). A related study by Yin P et al., 2004 (211) demonstrated a decreased copy number of mtDNA near the D-loop in HCC. In combination, these findings emphasize that alterations in the D-loop region represent important events during the early phase of liver carcinogenesis. Zhang R et al., 2010 illustrated the utility of single nucleotide polymorphisms (SNPs) and mutations in the mitochondria D-loop region for predicting the risk of HCC and for differentiating among HCCs with distinct etiologies (210).

4.3 Full- length mitochondrial sequence

In the coding region, we found 28 CCA and 19 HCC non-synonymous amino acids that were in the process of changing. On the other hand, disproportionate distributions of synonymous alterations were observed throughout the coding regions, involving all complexes (Table 3.1). The alteration in the *ND4L* gene of the metastasizing cell line, OZ, has also been identified at the margins with dysplasia adjacent to the primary head and neck tumor, suggesting that mitochondrial alteration may occur early in CCA tumors, prior to the appearance of the invasive phenotype (212). In cancer, synonymous mtDNA alterations can affect *in vivo* protein structures, therefore altering its functionality (213,214). Moreover, we found 11 non-synonymous alterations in Papova-immortalized normal hepatocyte cell line (THLE-3); however, it was unclear whether these alterations were observed because of true biological heteroplasmy

in liver cells, or was a molecular artifact of Papova- virus immortalization step and subsequent passaging required for producing normal hepatocyte cell lines.

Despite the presence of certain recurrent alterations, we were unable to find hot spot corresponding to many studies in pancreas cancer, such as *KRAS2* and *BRAF* (215,216). We compared the non-synonymous alterations that we had identified to the mitochondrial genome database (217); consequently, several of our reported alterations may exhibit a functional correlation with human diseases. Specifically, we found that G3407A has been associated with an uncommon variety of hypertrophy cardiomyopathy (218). Also, we detected an alteration in T12811C that might fulfill a potential modifier role in increasing the penetrance and expressivity of the primary Leber's hereditary optic neuropathy (LHON) (219).

Our study detected several non-synonymous alterations in specific locations that were reported in other cancers. For instance, we located A8701G, which was found in thyroid tumors (220). A10398G had been associated with invasive breast cancer and esophageal cancer in African American individuals (221,222). An identical alteration, G15756A, has been reported in human colonic crypt stem cells. This variation is important for understanding of the findings of mtDNA mutations in aging tissues and tumors as well as for determining the frequency of mtDNA mutations within a cell (223). Our novel non-synonymous alterations, A6678G, T9179Y, C10399S, G10401, T13277C, G15002A, T4759Y, A14756M and C14772Y might fulfill a function in carcinogenesis. For instance, the A6678G modification changes a moderately-conserved threonine residue to proline in *COI*. The alteration of T9179Y changes a highly conserved

hydrophobic valine to a hydrophilic alanine in *ATPase6*. Collectively, these non-synonymous alterations are potentially harmful because they occur in highly conserved sequence; therefore, they may affect the mitochondrial OXPHOS function.

The common deletion of the mitochondrial genome 4977-bp was not detected by the current array, MitoChip. Consequently, a more comprehensive analysis is required for examining this common deletion in CCA and HCC, since the variation may affect the mutational rate of normal and tumor tissues (211). In particular, Yin et al., 2004 (211) revealed a low frequency of mtDNA 4977-bp deletion in HCC as compared to the corresponding normal tissue. Such findings likely confirmed the contribution of the 4977 deletion in accumulating the two types of mtDNA mutations in HCC (211).

4.4 Quantification of mitochondrial genome levels

The low abundance of mtDNA has been reported in cancer tissues such as renal (140), gastric (224), breast (139) and hepatocellular carcinoma (211). Conversely, an increase in mtDNA content was shown in renal oncocytomas (225), head and neck cancer (144), endometrial cancer (226), ovarian cancer (227) and colorectal cancer (228). Interestingly, the total mtDNA copy numbers varied between hepatocellular carcinoma and paired non-neoplastic carcinoma. In particular, these differences depend on the background of the liver; hepatocellular carcinoma possesses fewer mtDNA in non-cirrhotic livers than it does in cirrhotic livers (141,211). The alteration of mtDNA content is specific to the type of cancer. Although the effects of these alterations on the carcinogenesis or the progression

of CCA and HCC are still obscure, these modifications have the potential to impair the function of the OXPHOS system in CCA and HCC. However, the underlying molecular mechanisms of the alterations in cancer cell mtDNA are considerably unclear.

4.5 Analysis of OXPHOS proteins associated with morphological, depolrziation and functional alterations

Other important findings in the present study sought to determine if the morphological alterations in the mitochondria could be correlated with perturbations of mitochondrial functioning. Accordingly, we measured the enzyme activities of Complexes I, II, II + III and IV from CCA and HCC cell lines. The concomitant reduction in the content of mitochondrial respiratory proteins strongly suggests that the biogenesis of mitochondria was repressed in CCA and HCC (119,229). In particular, these cell lines demonstrated a marked reduction of ubiquinol-cytochrome c reductase (Figure 3.4), which as the Rieske Fe-S protein, is a key subunit of cytochrome bc_1 (Complex III) in the respiratory chain complexes. This complex plays a crucial role in generating an electrochemical potential when the electrons transfer from ubiquinol to cytochrome *c* in order to synthesize ATP. Our findings, as demonstrated in Figure 3.6, are consistent with a previous study by Ohashi et al., 2004 (230). This study reported that the upregulation of Ubiquinol-cytochrome *c* reductase suggests the amplification of the Ubiquinol-cytochrome *c* reductase gene in variety of tumors along with the elevation of mitochondrial membrane potential ($\Delta\psi m$). Similarly, Warburg (1956) showed that cancer cells have a respiratory

deficiency that is associated with decreased numbers and reduced OXPHOS protein levels. Hence, our data support Warburg's study and also suggests that mitochondrial biogenesis is impaired during liver carcinogenesis (90). Most cancer cells have very high glycolytic rates that result in the excessive generation of lactate and NADH (Figure 3.7 and 3.8) (90,204,231), which are beyond the capacity of pyruvate dehydrogenase and NADH mitochondrial shuttle (232). The high NADH levels are caused by a disruption of the glycerol 3-phosphate shuttle and a reduction of glutaminolysis as found in breast cancer cell lines (MCF-7 cells) (117). Therefore, most cancer cells in culture produce higher quantity of lactate, implying that the net flow of the intracellular conversion shifts from pyruvate to lactate. This indicates a switch from mitochondrial oxidative phosphorylation to glycolysis from ATP production.

A previous study by Yin et al., 2004 (211) found that the overexpression of PGC-1 α, peroxisome proliferator-activated receptor gamma coactivator-1 alpha, strikingly decreased cell migration through the upregulation of E-cadherin expression in HepG2 cell lines. A study by our group Abuetabh Y et al., 2011 recently demonstrated that the CCA cell lines expressed the E-cad and β-catenin in different localization patterns. Collectively, these findings suggest that alterations of mtDNA and mitochondrial dysfunction may stimulate malignant progression in CCA and HCC (233).

In conclusion, mtDNA alterations are common in CCA. A high copy number of mtDNA mutations suggest that these alterations may contain promising fields of further investigation in CCA carcinogenesis and platforms for diagnostic

applications. Questions remain regarding the progression and functional implications of these mutations in the pathogenesis of CCA. Further studies in the molecular mechanisms of the mtDNA alterations and mitochondrial OXPHOS defects are required to provide insights into cancer progression and mitochondrial-targeted therapies.

4.6 Summary

Although CCA is one of the primary malignancies of the biliary tract, this cancer form has received less attention than hepatocellular carcinoma (HCC). Some primary and secondary cholangiopathies as well as chronic infections of the biliary tract are relatively common worldwide and have been identified as underlying precancerous lesions for the occurrence of CCA. Furthermore, somatic mitochondrial DNA (mtDNA) mutations have been demonstrated in a variety of human cancers. However, no study has previously targeted mitochondrial DNA alterations in CCA. In collaboration with international partners (Seattle, WA, USA), we conducted a preliminary analysis using MitoChip sequencing on mitochondrial DNA obtained from three CCA and two HCC cell lines. Western blot analysis and ultrastructural investigation with a transmission electron microscope were used to identify oxidative phosphorylation (OXPHOS) for respiratory protein content and mitochondrial cristae alterations. Moreover, real time quantitative PCR, confocal laser microscopy and metabolic assays including L-Lactate and NAD^+/NADH assays were used to identify mtDNA copy number, mitochondrial membrane potential measurements and metabolic differences, respectively. Among 106 mtDNA alterations observed in three CCA cell lines,

including OZ, HuCCT1 and Huh-28, 36 were non-synonymous coding region mutations that resulted in an amino acid change. Thirty-seven of these alterations were synonymous and 33 were involved in non-coding, including ribosomal RNA (rRNA) and transfer RNA (tRNA). Of the 76 mtDNA alterations observed in two HCC cell lines, HepG-2 and HuH-7, 27 alterations were non-synonymous coding region mutations, 27 variations were synonymous, and 22 mutations were involved in non-coding, including rRNA and tRNA. Moreover, significant decreases in Complexes I and III associated the morphological and polarization alterations, which more evident in CCA than HCC. Our findings suggest that mtDNA alterations are common in CCA. The relationship between anaerobic and aerobic metabolisms in the surrounding liver tissue may provide clues for studies investigating the epithelial-mesenchymal interaction and the host response. Microarray analysis with MitoChip as well as metabolomics may contribute significantly to identifying new carcinogenetic pathways that alter CCA. Future studies that provide additional information on these pathways will not only contribute to a better understanding of CCA carcinogenesis but will also assist in identifying patients with underlying disorders who progress to neoplastic transformation. Although some limitations may be considered, e.g. virus-induced immortalized cell lines that are not properly normal healthy hepatocytes, our study may be considered highly specific, because of the lack of contamination of both stromal and host lymphocytes that are usually present in studying tissue samples. Our study is considered to be significant in liver cancer research, as it increases the available knowledge about mtDNA and highlights some molecular

mechanisms possibly involved in carcinogenesis. This information is considered a gateway for further *in vivo* studies and identifying valuable therapeutic targets that can fulfill a role in minimizing the mortality rate of liver cancer patients.

4.7 Concluding Remarks

To the best of our knowledge, this study represents the first effort that targets a complete mitochondrial genome sequencing array in cholangiocarcinoma cell lines and the first investigation concerning the frequency of mitochondrial mutations using an array-based sequencing technology. Since the sequencing of the human genome was completed, the main goals of functional genomics have entailed determining the function of newly identified genes products and identifying the genes that might be therapeutically targeted. To date, genomics strategies have largely centered on gene expression studies, transcriptomics, or protein profiles, proteomics. Moreover, metabolic activity can be quantified, as various analytical tools have been developed to measure concentrations of low molecular weight metabolites. The use of microarray and metabolomics in cancer would significantly assist the diagnosis of cancer at an early stage as well as increase the chance of survival and the quality of life.

4.8 Future Directions

4.8.1 To scan the mitochondrial DNA (mtDNA) in a large scale of human samples, including quantifying the total mtDNA levels and quantifying the levels of mtDNA 4,977bp common deletion.

Preliminary results showed that mtDNA alterations are common in CCA. In that process we used the MitoChip array, comparing it with the revised

Cambridge Reference Sequence (rCRS) to evaluate nucleotide alterations. We aim to conduct MitoChip analysis in a panel of CCA tissue samples to produce deeper analyses. Moreover, despite the extensive studies in alteration of mtDNA qualitatively (mutations) and quantitatively (mtDNA copy number) in other different kind of cancers, the questions if the mtDNA copy number plays a role in progression of CCA still need to be addressed. The common deletion of the mitochondrial genome 4977-bp was not detected by the current array, MitoChip. Consequently, more comprehensive analysis is required for this common deletion in CCA and HCC, since it may affect the mutational rate of normal and tumor tissues (234). In particular, Yin et al. 2004 revealed a low frequency of mtDNA 4977-bp deletion in HCC as compared to corresponding normal tissue. Those findings likely confirmed the contribution of the 4977 deletion in accumulating the two types of mtDNA mutations in HCC (234).

4.8.2 To assess the mitochondrial bioenergetics alterations in CCA cells and their correlation with mitochondrial function including measurement of ATP content and O_2 consumption.

Normally, most cells convert glucose to pyruvate through pyruvate oxidation in order to produce ATP. The oxidative phosphorylation system (OXPHOS) within mitochondria utilize electron flow from reduced substrates to molecular oxygen to synthesize ATP. However, in the absence of oxygen, pyruvate is converted to lactate in the cytoplasm, thus completing the glycolysis cycle. Conversion of glucose into lactate under normal oxygen tension, a distinct characteristic of tumor cells, is also known as aerobic glycolysis. From the

physiological and alteration stand points of the cells, a parameter can be measured via evaluating Oxygen Consumption Rate (OCR) as an indicator of mitochondrial respiration. The measurement of lactate produced indirectly via protons released into the extracellular medium surrounding the cells, causing acidification of the medium, provides the Extracellular Acidification Rate (ECAR). These bioenergetics alterations associated with malignant transformation are being exploited to identify potential cancer-selective therapeutics.

4.8.3 To analyze the correlation between p53 status and mtDNA mutation in CCA cell lines and patient samples.

P53 system has been almost a target protein for studying cancer. More attention has been given to this protein when almost all human cancer showed either mutation in this protein that inhibited their activity or even dysfunctional activity. Although p53 performs its main role in the mitochondrial outer membrane it also interacts with different proteins in the mitochondrial inner membrane and matrix. Several studies support findings of an increased p53 mutational load and its association with an increased level of oxy-radical species (203,235).

References

(1) Ernster L, Schatz G. Mitochondria: a historical review. J Cell Biol 1981 Dec 20;91(3 Pt 2):227s-255s.

(2) PALADE GE. The fine structure of mitochondria. Anat Rec 1952 Nov 1;114(3):427-451.

(3) NOVIKOFF AB, SHIN WY, DRUCKER J. Mitochondrial localization of oxidative enzymes: staining results with two tetrazolium salts. J Biophys Biochem Cytol 1961 Jan 12;9:47-61.

(4) Gilkerson RW, Selker JM, Capaldi RA. The cristal membrane of mitochondria is the principal site of oxidative phosphorylation. FEBS Lett 2003 Jul 10;546(2-3):355-358.

(5) Mannella CA. Structure and dynamics of the mitochondrial inner membrane cristae. Biochim Biophys Acta 2006 May 12;1763(5-6):542-548.

(6) Smeitink JAM, Sengers RCA, Trijbels JMF. Oxidative phosphorylation in health and disease. Georgetown, Tex., U.S.A; New York, N.Y., U.S.A: Landes Bioscience/Eurekah.com; Kluwer Academic/Plenum Publishers; 2004.

(7) MITOMAP. Available at: http://www.mitomap.org/MITOMAP.

(8) Anderson S, Bankier AT, Barrell BG, de Bruijn MH, Coulson AR, Drouin J, et al. Sequence and organization of the human mitochondrial genome. Nature 1981 Apr 9;290(5806):457-465.

(9) Taanman JW. The mitochondrial genome: structure, transcription, translation and replication. Biochim Biophys Acta 1999 Feb 9;1410(2):103-123.

(10) Wallace DC, Brown MD, Lott MT. Mitochondrial DNA variation in human evolution and disease. Gene 1999 Sep 30;238(1):211-230.

(11) Taanman JW. The mitochondrial genome: structure, transcription, translation and replication. Biochim Biophys Acta 1999 Feb 9;1410(2):103-123.

(12) Fernandez-Silva P, Enriquez JA, Montoya J. Replication and transcription of mammalian mitochondrial DNA. Exp Physiol 2003 Jan 8;88(1):41-56.

(13) Madsen CS, Ghivizzani SC, Hauswirth WW. Protein binding to a single termination-associated sequence in the mitochondrial DNA D-loop region. Mol Cell Biol 1993 Apr 14;13(4):2162-2171.

(14) Giles RE, Blanc H, Cann HM, Wallace DC. Maternal inheritance of human mitochondrial DNA. Proc Natl Acad Sci U S A 1980 Nov 16;77(11):6715-6719.

(15) Cann RL, Stoneking M, Wilson AC. Mitochondrial DNA and human evolution. Nature 1987 Jan 7;325(6099):31-36.

(16) Sohal RS, Dubey A. Mitochondrial oxidative damage, hydrogen peroxide release, and aging. Free Radic Biol Med 1994 May 19;16(5):621-626.

(17) Ricci JE, Waterhouse N, Green DR. Mitochondrial functions during cell death, a complex (I-V) dilemma. Cell Death Differ 2003 May 16;10(5):488-492.

(18) Schagger H, Pfeiffer K. The ratio of oxidative phosphorylation complexes I-V in bovine heart mitochondria and the composition of respiratory chain supercomplexes. J Biol Chem 2001 Oct 12;276(41):37861-37867.

(19) Carroll J, Shannon RJ, Fearnley IM, Walker JE, Hirst J. Definition of the nuclear encoded protein composition of bovine heart mitochondrial complex I. Identification of two new subunits. J Biol Chem 2002 Dec 27;277(52):50311-50317.

(20) Chen X, Qi F, Dash RK, Beard DA. Kinetics and regulation of mammalian NADH-ubiquinone oxidoreductase (Complex I). Biophys J 2010 Sep 8;99(5):1426-1436.

(21) Nelsestuen GL. Amino acid-directed nucleic acid synthesis. A possible mechanism in the origin of life. J Mol Evol 1978 Jun 20;11(2):109-120.

(22) Horton TM, Petros JA, Heddi A, Shoffner J, Kaufman AE, Graham SD,Jr, et al. Novel mitochondrial DNA deletion found in a renal cell carcinoma. Genes Chromosomes Cancer 1996 Feb 13;15(2):95-101.

(23) Gonzalo R, Garcia-Arumi E, Llige D, Marti R, Solano A, Montoya J, et al. Free radicals-mediated damage in transmitochondrial cells harboring the T14487C mutation in the ND6 gene of mtDNA. FEBS Lett 2005 Dec 19;579(30):6909-6913.

(24) Ishikawa K, Takenaga K, Akimoto M, Koshikawa N, Yamaguchi A, Imanishi H, et al. ROS-generating mitochondrial DNA mutations can regulate tumor cell metastasis. Science 2008 May 2;320(5876):661-664.

(25) Schafer E, Seelert H, Reifschneider NH, Krause F, Dencher NA, Vonck J. Architecture of active mammalian respiratory chain supercomplexes. J Biol Chem 2006 Jun 2;281(22):15370-15375.

(26) Lenaz G, Genova ML. Kinetics of integrated electron transfer in the mitochondrial respiratory chain: random collisions vs. solid state electron channeling. Am J Physiol Cell Physiol 2007 Apr 14;292(4):C1221-39.

(27) Mitchell P. The protonmotive Q cycle: a general formulation. FEBS Lett 1975 Nov 15;59(2):137-139.

(28) McCulloch V, Seidel-Rogol BL, Shadel GS. A human mitochondrial transcription factor is related to RNA adenine methyltransferases and binds S-adenosylmethionine. Mol Cell Biol 2002 Feb 2;22(4):1116-1125.

(29) Dasgupta S, Hoque MO, Upadhyay S, Sidransky D. Mitochondrial cytochrome B gene mutation promotes tumor growth in bladder cancer. Cancer Res 2008 Feb 1;68(3):700-706.

(30) Tsukihara T, Aoyama H, Yamashita E, Tomizaki T, Yamaguchi H, Shinzawa-Itoh K, et al. Structures of metal sites of oxidized bovine heart cytochrome c oxidase at 2.8 A. Science 1995 Aug 25;269(5227):1069-1074.

(31) Fontanesi F, Soto IC, Horn D, Barrientos A. Assembly of mitochondrial cytochrome c-oxidase, a complicated and highly regulated cellular process. Am J Physiol Cell Physiol 2006 Dec 19;291(6):C1129-47.

(32) Zhu J, Han H, Pawate A, Gennis RB. Decoupling mutations in the D-channel of the aa(3)-type cytochrome c oxidase from Rhodobacter sphaeroides suggest that a continuous hydrogen-bonded chain of waters is essential for proton pumping. Biochemistry 2010 Jun 1;49(21):4476-4482.

(33) Wikstrom M, Jasaitis A, Backgren C, Puustinen A, Verkhovsky MI. The role of the D- and K-pathways of proton transfer in the function of the haem-copper oxidases. Biochim Biophys Acta 2000 Aug 15;1459(2-3):514-520.

(34) Nelson DL, Lehninger AL, Cox MM. Lehninger principles of biochemistry. 5th ed. New York: W.H. Freeman; 2008.

(35) Michel H. Cytochrome c oxidase: catalytic cycle and mechanisms of proton pumping--a discussion. Biochemistry 1999 Nov 16;38(46):15129-15140.

(36) Coenen MJ, van den Heuvel LP, Ugalde C, Ten Brinke M, Nijtmans LG, Trijbels FJ, et al. Cytochrome c oxidase biogenesis in a patient with a mutation in COX10 gene. Ann Neurol 2004 Oct 15;56(4):560-564.

(37) Fernandez-Vizarra E, Tiranti V, Zeviani M. Assembly of the oxidative phosphorylation system in humans: what we have learned by studying its defects. Biochim Biophys Acta 2009 Jan 1;1793(1):200-211.

(38) Gasparre G, Porcelli AM, Bonora E, Pennisi LF, Toller M, Iommarini L, et al. Disruptive mitochondrial DNA mutations in complex I subunits are markers of oncocytic phenotype in thyroid tumors. Proc Natl Acad Sci U S A 2007 May 22;104(21):9001-9006.

(39) Cavelier L, Jazin EE, Eriksson I, Prince J, Bave U, Oreland L, et al. Decreased cytochrome-c oxidase activity and lack of age-related accumulation of mitochondrial DNA deletions in the brains of schizophrenics. Genomics 1995 Sep 1;29(1):217-224.

(40) Sun AS, Cederbaum AI. Oxidoreductase activities in normal rat liver, tumor-bearing rat liver, and hepatoma HC-252. Cancer Res 1980 Dec 3;40(12):4677-4681.

(41) Abril J, de Heredia ML, Gonzalez L, Cleries R, Nadal M, Condom E, et al. Altered expression of 12S/MT-RNR1, MT-CO2/COX2, and MT-ATP6 mitochondrial genes in prostate cancer. Prostate 2008 Jul 1;68(10):1086-1096.

(42) Heerdt BG, Halsey HK, Lipkin M, Augenlicht LH. Expression of mitochondrial cytochrome c oxidase in human colonic cell differentiation, transformation, and risk for colonic cancer. Cancer Res 1990 Mar 1;50(5):1596-1600.

(43) Guzman JN, Sanchez-Padilla J, Wokosin D, Kondapalli J, Ilijic E, Schumacker PT, et al. Oxidant stress evoked by pacemaking in dopaminergic neurons is attenuated by DJ-1. Nature 2010 Dec 2;468(7324):696-700.

(44) Ong SB, Subrayan S, Lim SY, Yellon DM, Davidson SM, Hausenloy DJ. Inhibiting mitochondrial fission protects the heart against ischemia/reperfusion injury. Circulation 2010 May 11;121(18):2012-2022.

(45) Carelli V, Ross-Cisneros FN, Sadun AA. Optic nerve degeneration and mitochondrial dysfunction: genetic and acquired optic neuropathies. Neurochem Int 2002 May 23;40(6):573-584.

(46) Dionisi-Vici C, Seneca S, Zeviani M, Fariello G, Rimoldi M, Bertini E, et al. Fulminant Leigh syndrome and sudden unexpected death in a family with the T9176C mutation of the mitochondrial ATPase 6 gene. J Inherit Metab Dis 1998 Feb 20;21(1):2-8.

(47) Arnold RS, Sun CQ, Richards JC, Grigoriev G, Coleman IM, Nelson PS, et al. Mitochondrial DNA mutation stimulates prostate cancer growth in bone stromal environment. Prostate 2009 Jan 1;69(1):1-11.

(48) Shidara Y, Yamagata K, Kanamori T, Nakano K, Kwong JQ, Manfredi G, et al. Positive contribution of pathogenic mutations in the mitochondrial genome to

the promotion of cancer by prevention from apoptosis. Cancer Res 2005 Mar 1;65(5):1655-1663.

(49) Chance B, Sies H, Boveris A. Hydroperoxide metabolism in mammalian organs. Physiol Rev 1979 Jul 23;59(3):527-605.

(50) Turrens JF, Boveris A. Generation of superoxide anion by the NADH dehydrogenase of bovine heart mitochondria. Biochem J 1980 Nov 1;191(2):421-427.

(51) Turrens JF. Mitochondrial formation of reactive oxygen species. J Physiol 2003 Oct 15;552(Pt 2):335-344.

(52) Muller FL, Liu Y, Van Remmen H. Complex III releases superoxide to both sides of the inner mitochondrial membrane. J Biol Chem 2004 Nov 19;279(47):49064-49073.

(53) McCord JM, Fridovich I. Superoxide dismutase. An enzymic function for erythrocuprein (hemocuprein). J Biol Chem 1969 Nov 25;244(22):6049-6055.

(54) Oberley LW. Anticancer therapy by overexpression of superoxide dismutase. Antioxid Redox Signal 2001 Jun 21;3(3):461-472.

(55) Rao GN. Hydrogen peroxide induces complex formation of SHC-Grb2-SOS with receptor tyrosine kinase and activates Ras and extracellular signal-regulated protein kinases group of mitogen-activated protein kinases. Oncogene 1996 Aug 15;13(4):713-719.

(56) Mercurio F, Manning AM. NF-kappaB as a primary regulator of the stress response. Oncogene 1999 Nov 1;18(45):6163-6171.

(57) Adler V, Yin Z, Fuchs SY, Benezra M, Rosario L, Tew KD, et al. Regulation of JNK signaling by GSTp. EMBO J 1999 Mar 1;18(5):1321-1334.

(58) Vinogradov AD, Grivennikova VG. Generation of superoxide-radical by the NADH:ubiquinone oxidoreductase of heart mitochondria. Biochemistry (Mosc) 2005 Feb 24;70(2):120-127.

(59) Cohen G, Farooqui R, Kesler N. Parkinson disease: a new link between monoamine oxidase and mitochondrial electron flow. Proc Natl Acad Sci U S A 1997 May 13;94(10):4890-4894.

(60) Emerit I. Reactive oxygen species, chromosome mutation, and cancer: possible role of clastogenic factors in carcinogenesis. Free Radic Biol Med 1994 Jan 12;16(1):99-109.

(61) Petros JA, Baumann AK, Ruiz-Pesini E, Amin MB, Sun CQ, Hall J, et al. mtDNA mutations increase tumorigenicity in prostate cancer. Proc Natl Acad Sci U S A 2005 Jan 18;102(3):719-724.

(62) Papandreou I, Cairns RA, Fontana L, Lim AL, Denko NC. HIF-1 mediates adaptation to hypoxia by actively downregulating mitochondrial oxygen consumption. Cell Metab 2006 Mar 3;3(3):187-197.

(63) Kim JW, Tchernyshyov I, Semenza GL, Dang CV. HIF-1-mediated expression of pyruvate dehydrogenase kinase: a metabolic switch required for cellular adaptation to hypoxia. Cell Metab 2006 Mar 23;3(3):177-185.

(64) Lu CW, Lin SC, Chen KF, Lai YY, Tsai SJ. Induction of pyruvate dehydrogenase kinase-3 by hypoxia-inducible factor-1 promotes metabolic switch and drug resistance. J Biol Chem 2008 Oct 17;283(42):28106-28114.

(65) Dang CV, Le A, Gao P. MYC-induced cancer cell energy metabolism and therapeutic opportunities. Clin Cancer Res 2009 Nov 1;15(21):6479-6483.

(66) Kim JW, Gao P, Liu YC, Semenza GL, Dang CV. Hypoxia-inducible factor 1 and dysregulated c-Myc cooperatively induce vascular endothelial growth factor and metabolic switches hexokinase 2 and pyruvate dehydrogenase kinase 1. Mol Cell Biol 2007 Nov 14;27(21):7381-7393.

(67) Dang CV, Kim JW, Gao P, Yustein J. The interplay between MYC and HIF in cancer. Nat Rev Cancer 2008 Jan 25;8(1):51-56.

(68) Veeramani S, Yuan TC, Lin FF, Lin MF. Mitochondrial redox signaling by p66Shc is involved in regulating androgenic growth stimulation of human prostate cancer cells. Oncogene 2008 Aug 28;27(37):5057-5068.

(69) Pani G, Koch OR, Galeotti T. The p53-p66shc-Manganese Superoxide Dismutase (MnSOD) network: a mitochondrial intrigue to generate reactive oxygen species. Int J Biochem Cell Biol 2009 May 27;41(5):1002-1005.

(70) Trinei M, Giorgio M, Cicalese A, Barozzi S, Ventura A, Migliaccio E, et al. A p53-p66Shc signalling pathway controls intracellular redox status, levels of oxidation-damaged DNA and oxidative stress-induced apoptosis. Oncogene 2002 May 30;21(24):3872-3878.

(71) Starkov AA. The role of mitochondria in reactive oxygen species metabolism and signaling. Ann N Y Acad Sci 2008 Dec 17;1147:37-52.

(72) Circu ML, Aw TY. Reactive oxygen species, cellular redox systems, and apoptosis. Free Radic Biol Med 2010 Mar 15;48(6):749-762.

(73) Oberley TD, Oberley LW. Antioxidant enzyme levels in cancer. Histol Histopathol 1997 Apr 23;12(2):525-535.

(74) Wyllie AH. Apoptosis: an overview. Br Med Bull 1997;53(3):451-465.

(75) Oberhammer F, Wilson JW, Dive C, Morris ID, Hickman JA, Wakeling AE, et al. Apoptotic death in epithelial cells: cleavage of DNA to 300 and/or 50 kb fragments prior to or in the absence of internucleosomal fragmentation. EMBO J 1993 Sep 24;12(9):3679-3684.

(76) Wyllie AH. Glucocorticoid-induced thymocyte apoptosis is associated with endogenous endonuclease activation. Nature 1980 Apr 10;284(5756):555-556.

(77) Igney FH, Krammer PH. Death and anti-death: tumour resistance to apoptosis. Nat Rev Cancer 2002 Apr 27;2(4):277-288.

(78) Hockenbery DM, Oltvai ZN, Yin XM, Milliman CL, Korsmeyer SJ. Bcl-2 functions in an antioxidant pathway to prevent apoptosis. Cell 1993 Oct 22;75(2):241-251.

(79) Yang J, Liu X, Bhalla K, Kim CN, Ibrado AM, Cai J, et al. Prevention of apoptosis by Bcl-2: release of cytochrome c from mitochondria blocked. Science 1997 Feb 21;275(5303):1129-1132.

(80) Lemasters JJ, Nieminen AL, Qian T, Trost LC, Elmore SP, Nishimura Y, et al. The mitochondrial permeability transition in cell death: a common mechanism in necrosis, apoptosis and autophagy. Biochim Biophys Acta 1998 Aug 10;1366(1-2):177-196.

(81) Miyashita T, Reed JC. Tumor suppressor p53 is a direct transcriptional activator of the human bax gene. Cell 1995 Jan 27;80(2):293-299.

(82) Mihara M, Erster S, Zaika A, Petrenko O, Chittenden T, Pancoska P, et al. P53 has a Direct Apoptogenic Role at the Mitochondria. Mol Cell 2003 Mar 12;11(3):577-590.

(83) Leung AW, Halestrap AP. Recent progress in elucidating the molecular mechanism of the mitochondrial permeability transition pore. Biochim Biophys Acta 2008 Jul-Aug 25;1777(7-8):946-952.

(84) Leung AW, Varanyuwatana P, Halestrap AP. The mitochondrial phosphate carrier interacts with cyclophilin D and may play a key role in the permeability transition. J Biol Chem 2008 Sep 26;283(39):26312-26323.

(85) Du C, Fang M, Li Y, Li L, Wang X. Smac, a mitochondrial protein that promotes cytochrome c-dependent caspase activation by eliminating IAP inhibition. Cell 2000 Jul 7;102(1):33-42.

(86) Hill MM, Adrain C, Martin SJ. Portrait of a killer: the mitochondrial apoptosome emerges from the shadows. Mol Interv 2003 Feb 30;3(1):19-26.

(87) Tenev T, Zachariou A, Wilson R, Ditzel M, Meier P. IAPs are functionally non-equivalent and regulate effector caspases through distinct mechanisms. Nat Cell Biol 2005 Jan 17;7(1):70-77.

(88) Alberts B, Keyano. Molecular biology of the cell. Reference edition. New York, NY: Garland Science; 2008.

(89) Racker E. History of the Pasteur effect and its pathobiology. Mol Cell Biochem 1974 Nov 15;5(1-2):17-23.

(90) WARBURG O. On the origin of cancer cells. Science 1956 Feb 24;123(3191):309-314.

(91) Matoba S, Kang JG, Patino WD, Wragg A, Boehm M, Gavrilova O, et al. P53 Regulates Mitochondrial Respiration. Science 2006 Jun 16;312(5780):1650-1653.

(92) Fantin VR, St-Pierre J, Leder P. Attenuation of LDH-A expression uncovers a link between glycolysis, mitochondrial physiology, and tumor maintenance. Cancer Cell 2006 Jun 24;9(6):425-434.

(93) Bui T, Thompson CB. Cancer's sweet tooth. Cancer Cell 2006 Jun 28;9(6):419-420.

(94) Kim JW, Dang CV. Cancer's molecular sweet tooth and the Warburg effect. Cancer Res 2006 Sep 15;66(18):8927-8930.

(95) Shibanuma M, Kuroki T, Nose K. Superoxide as a signal for increase in intracellular pH. J Cell Physiol 1988 Aug 18;136(2):379-383.

(96) Ikebuchi Y, Masumoto N, Tasaka K, Koike K, Kasahara K, Miyake A, et al. Superoxide anion increases intracellular pH, intracellular free calcium, and arachidonate release in human amnion cells. J Biol Chem 1991 Jul 15;266(20):13233-13237.

(97) Lopez-Lazaro M. HIF-1: hypoxia-inducible factor or dysoxia-inducible factor? FASEB J 2006 May 20;20(7):828-832.

(98) Brunelle JK, Bell EL, Quesada NM, Vercauteren K, Tiranti V, Zeviani M, et al. Oxygen sensing requires mitochondrial ROS but not oxidative phosphorylation. Cell Metab 2005 Jun 26;1(6):409-414.

(99) Seagroves TN, Ryan HE, Lu H, Wouters BG, Knapp M, Thibault P, et al. Transcription factor HIF-1 is a necessary mediator of the pasteur effect in mammalian cells. Mol Cell Biol 2001 May 13;21(10):3436-3444.

(100) Semenza GL. HIF-1 mediates the Warburg effect in clear cell renal carcinoma. J Bioenerg Biomembr 2007 Jun 17;39(3):231-234.

(101) Ferdinandy P, Schulz R. Nitric oxide, superoxide, and peroxynitrite in myocardial ischaemia-reperfusion injury and preconditioning. Br J Pharmacol 2003 Feb 28;138(4):532-543.

(102) Dang CV, Semenza GL. Oncogenic alterations of metabolism. Trends Biochem Sci 1999 Feb 13;24(2):68-72.

(103) Elstrom RL, Bauer DE, Buzzai M, Karnauskas R, Harris MH, Plas DR, et al. Akt stimulates aerobic glycolysis in cancer cells. Cancer Res 2004 Jun 1;64(11):3892-3899.

(104) Reshkin SJ, Bellizzi A, Caldeira S, Albarani V, Malanchi I, Poignee M, et al. Na+/H+ exchanger-dependent intracellular alkalinization is an early event in malignant transformation and plays an essential role in the development of subsequent transformation-associated phenotypes. FASEB J 2000 Nov 14;14(14):2185-2197.

(105) Harguindey S, Orive G, Luis Pedraz J, Paradiso A, Reshkin SJ. The role of pH dynamics and the Na+/H+ antiporter in the etiopathogenesis and treatment of cancer. Two faces of the same coin--one single nature. Biochim Biophys Acta 2005 Sep 25;1756(1):1-24.

(106) Cardone RA, Casavola V, Reshkin SJ. The role of disturbed pH dynamics and the Na+/H+ exchanger in metastasis. Nat Rev Cancer 2005 Oct 23;5(10):786-795.

(107) Cuezva JM, Krajewska M, de Heredia ML, Krajewski S, Santamaria G, Kim H, et al. The bioenergetic signature of cancer: a marker of tumor progression. Cancer Res 2002 Nov 15;62(22):6674-6681.

(108) DiMauro S, Schon EA. Mitochondrial DNA mutations in human disease. Am J Med Genet 2001 Spring;106(1):18-26.

(109) Vu TH, Hirano M, DiMauro S. Mitochondrial diseases. Neurol Clin 2002 Aug 26;20(3):809-39, vii-viii.

(110) Clayton DA, Vinograd J. Complex mitochondrial DNA in leukemic and normal human myeloid cells. Proc Natl Acad Sci U S A 1969 Apr 4;62(4):1077-1084.

(111) Ye C, Shu XO, Pierce L, Wen W, Courtney R, Gao YT, et al. Mutations in the mitochondrial DNA D-loop region and breast cancer risk. Breast Cancer Res Treat 2010 Jan 11;119(2):431-436.

(112) Mambo E, Gao X, Cohen Y, Guo Z, Talalay P, Sidransky D. Electrophile and oxidant damage of mitochondrial DNA leading to rapid evolution of homoplasmic mutations. Proc Natl Acad Sci U S A 2003 Feb 18;100(4):1838-1843.

(113) Burgart LJ, Zheng J, Shu Q, Strickler JG, Shibata D. Somatic mitochondrial mutation in gastric cancer. Am J Pathol 1995 Oct 19;147(4):1105-1111.

(114) Liu VW, Shi HH, Cheung AN, Chiu PM, Leung TW, Nagley P, et al. High incidence of somatic mitochondrial DNA mutations in human ovarian carcinomas. Cancer Res 2001 Aug 15;61(16):5998-6001.

(115) Zhao YB, Yang HY, Zhang XW, Chen GY. Mutation in D-loop region of mitochondrial DNA in gastric cancer and its significance. World J Gastroenterol 2005 Jun 7;11(21):3304-3306.

(116) Nomoto S, Yamashita K, Koshikawa K, Nakao A, Sidransky D. Mitochondrial D-loop mutations as clonal markers in multicentric hepatocellular carcinoma and plasma. Clin Cancer Res 2002 Feb 8;8(2):481-487.

(117) Chatterjee A, Mambo E, Sidransky D. Mitochondrial DNA mutations in human cancer. Oncogene 2006 Aug 7;25(34):4663-4674.

(118) Chatterjee A, Dasgupta S, Sidransky D. Mitochondrial subversion in cancer. Cancer Prev Res (Phila) 2011 May 7;4(5):638-654.

(119) Lu J, Sharma LK, Bai Y. Implications of mitochondrial DNA mutations and mitochondrial dysfunction in tumorigenesis. Cell Res 2009 Jul 20;19(7):802-815.

(120) Wong LJ. Pathogenic mitochondrial DNA mutations in protein-coding genes. Muscle Nerve 2007 Sep 29;36(3):279-293.

(121) De Paepe B, De Bleecker JL, Van Coster R. Histochemical methods for the diagnosis of mitochondrial diseases. Curr Protoc Hum Genet 2009 Oct 18;Chapter 19:Unit19.2.

(122) Scaglia F, Wong LJ. Human mitochondrial transfer RNAs: role of pathogenic mutation in disease. Muscle Nerve 2008 Feb 12;37(2):150-171.

(123) Ueki I, Koga Y, Povalko N, Akita Y, Nishioka J, Yatsuga S, et al. Mitochondrial tRNA gene mutations in patients having mitochondrial disease with lactic acidosis. Mitochondrion 2006 Feb 24;6(1):29-36.

(124) Anderson S, Bankier AT, Barrell BG, de Bruijn MH, Coulson AR, Drouin J, et al. Sequence and organization of the human mitochondrial genome. Nature 1981 Apr 9;290(5806):457-465.

(125) Wong LJ, Chen TJ, Tan DJ. Detection of mitochondrial DNA mutations using temporal temperature gradient gel electrophoresis. Electrophoresis 2004 Aug 28;25(15):2602-2610.

(126) Cutler DJ, Zwick ME, Carrasquillo MM, Yohn CT, Tobin KP, Kashuk C, et al. High-throughput variation detection and genotyping using microarrays. Genome Res 2001 Nov 11;11(11):1913-1925.

(127) Polyak K, Li Y, Zhu H, Lengauer C, Willson JK, Markowitz SD, et al. Somatic mutations of the mitochondrial genome in human colorectal tumours. Nat Genet 1998 Nov 23;20(3):291-293.

(128) Taylor RW, Barron MJ, Borthwick GM, Gospel A, Chinnery PF, Samuels DC, et al. Mitochondrial DNA mutations in human colonic crypt stem cells. J Clin Invest 2003 Nov 29;112(9):1351-1360.

(129) Fliss MS, Usadel H, Caballero OL, Wu L, Buta MR, Eleff SM, et al. Facile detection of mitochondrial DNA mutations in tumors and bodily fluids. Science 2000 Mar 17;287(5460):2017-2019.

(130) Gochhait S, Bhatt A, Sharma S, Singh YP, Gupta P, Bamezai RN. Concomitant presence of mutations in mitochondrial genome and p53 in cancer development - a study in north Indian sporadic breast and esophageal cancer patients. Int J Cancer 2008 Dec 1;123(11):2580-2586.

(131) Jakupciak JP, Maggrah A, Maragh S, Maki J, Reguly B, Maki K, et al. Facile whole mitochondrial genome resequencing from nipple aspirate fluid using MitoChip v2.0. BMC Cancer 2008 Apr 10; 18 (2):8-95.

(132) Mithani SK, Taube JM, Zhou S, Smith IM, Koch WM, Westra WH, et al. Mitochondrial mutations are a late event in the progression of head and neck squamous cell cancer. Clin Cancer Res 2007 Aug 1;13(15 Pt 1):4331-4335.

(133) Prior SL, Griffiths AP, Baxter JM, Baxter PW, Hodder SC, Silvester KC, et al. Mitochondrial DNA mutations in oral squamous cell carcinoma. Carcinogenesis 2006 May 20;27(5):945-950.

(134) He L, Luo L, Proctor SJ, Middleton PG, Blakely EL, Taylor RW, et al. Somatic mitochondrial DNA mutations in adult-onset leukaemia. Leukemia 2003 Dec 12;17(12):2487-2491.

(135) Jin X, Zhang J, Gao Y, Ding K, Wang N, Zhou D, et al. Relationship between mitochondrial DNA mutations and clinical characteristics in human lung cancer. Mitochondrion 2007 Sep 23;7(5):347-353.

(136) Abu-Amero KK, Alzahrani AS, Zou M, Shi Y. Association of mitochondrial DNA transversion mutations with familial medullary thyroid carcinoma/multiple endocrine neoplasia type 2 syndrome. Oncogene 2006 Feb 2;25(5):677-684.

(137) Maximo V, Soares P, Lima J, Cameselle-Teijeiro J, Sobrinho-Simoes M. Mitochondrial DNA somatic mutations (point mutations and large deletions) and mitochondrial DNA variants in human thyroid pathology: a study with emphasis on Hurthle cell tumors. Am J Pathol 2002 May 25;160(5):1857-1865.

(138) Zhou S, Kassauei K, Cutler DJ, Kennedy GC, Sidransky D, Maitra A, et al. An oligonucleotide microarray for high-throughput sequencing of the mitochondrial genome. J Mol Diagn 2006 Sep 21;8(4):476-482.

(139) Mambo E, Chatterjee A, Xing M, Tallini G, Haugen BR, Yeung SC, et al. Tumor-specific changes in mtDNA content in human cancer. Int J Cancer 2005 Oct 10;116(6):920-924.

(140) Xing J, Chen M, Wood CG, Lin J, Spitz MR, Ma J, et al. Mitochondrial DNA content: its genetic heritability and association with renal cell carcinoma. J Natl Cancer Inst 2008 Aug 6;100(15):1104-1112.

(141) Lee HC, Li SH, Lin JC, Wu CC, Yeh DC, Wei YH. Somatic mutations in the D-loop and decrease in the copy number of mitochondrial DNA in human hepatocellular carcinoma. Mutat Res 2004 Mar 22;547(1-2):71-78.

(142) Wu CC, Alper OM, Lu JF, Wang SP, Guo L, Chiang HS, et al. Mutation spectrum of the CFTR gene in Taiwanese patients with congenital bilateral absence of the vas deferens. Hum Reprod 2005 Sep 20;20(9):2470-2475.

(143) Simonnet H, Alazard N, Pfeiffer K, Gallou C, Beroud C, Demont J, et al. Low mitochondrial respiratory chain content correlates with tumor aggressiveness in renal cell carcinoma. Carcinogenesis 2002 May 24;23(5):759-768.

(144) Kim MM, Clinger JD, Masayesva BG, Ha PK, Zahurak ML, Westra WH, et al. Mitochondrial DNA quantity increases with histopathologic grade in premalignant and malignant head and neck lesions. Clin Cancer Res 2004 Dec 15;10(24):8512-8515.

(145) Rogounovitch TI, Saenko VA, Shimizu-Yoshida Y, Abrosimov AY, Lushnikov EF, Roumiantsev PO, et al. Large deletions in mitochondrial DNA in radiation-associated human thyroid tumors. Cancer Res 2002 Dec 1;62(23):7031-7041.

(146) Bonner MR, Shen M, Liu CS, Divita M, He X, Lan Q. Mitochondrial DNA content and lung cancer risk in Xuan Wei, China. Lung Cancer 2009 Mar 29;63(3):331-334.

(147) Lan Q, Lim U, Liu CS, Weinstein SJ, Chanock S, Bonner MR, et al. A prospective study of mitochondrial DNA copy number and risk of non-Hodgkin lymphoma. Blood 2008 Nov 15;112(10):4247-4249.

(148) Rohlena J, Dong LF, Ralph SJ, Neuzil J. Anticancer drugs targeting the mitochondrial electron transport chain. Antioxid Redox Signal 2011 Dec 15;15(12):2951-2974.

(149) Bonnet S, Archer SL, Allalunis-Turner J, Haromy A, Beaulieu C, Thompson R, et al. A mitochondria-K+ channel axis is suppressed in cancer and its normalization promotes apoptosis and inhibits cancer growth. Cancer Cell 2007 Jan 14;11(1):37-51.

(150) Blonski W, Kotlyar DS, Forde KA. Non-viral causes of hepatocellular carcinoma. World J Gastroenterol 2010 Aug 7;16(29):3603-3615.

(151) Taniguchi K, Roberts LR, Aderca IN, Dong X, Qian C, Murphy LM, et al. Mutational spectrum of beta-catenin, AXIN1, and AXIN2 in hepatocellular carcinomas and hepatoblastomas. Oncogene 2002 Jul 18;21(31):4863-4871.

(152) Motola-Kuba D, Zamora-Valdes D, Uribe M, Mendez-Sanchez N. Hepatocellular carcinoma. An overview. Ann Hepatol 2006 Jan-Mar 23;5(1):16-24.

(153) Nissen NN, Martin P. Hepatocellular carcinoma: the high-risk patient. J Clin Gastroenterol 2002 Nov-Dec 12;35(5 Suppl 2):S79-85.

(154) Stal P, Hultcrantz R, Moller L, Eriksson LC. The effects of dietary iron on initiation and promotion in chemical hepatocarcinogenesis. Hepatology 1995 Feb 16;21(2):521-528.

(155) Kelly JK, Davies JS, Jones AW. Alpha-1-antitrypsin deficiency and hepatocellular carcinoma. J Clin Pathol 1979 Apr 24;32(4):373-376.

(156) Leong TY, Leong AS. Epidemiology and carcinogenesis of hepatocellular carcinoma. HPB (Oxford) 2005 May 29;7(1):5-15.

(157) de Groen PC, Gores GJ, LaRusso NF, Gunderson LL, Nagorney DM. Biliary tract cancers. N Engl J Med 1999 Oct 28;341(18):1368-1378.

(158) Mosconi S, Beretta GD, Labianca R, Zampino MG, Gatta G, Heinemann V. Cholangiocarcinoma. Crit Rev Oncol Hematol 2009 Mar 23;69(3):259-270.

(159) Gatto M, Bragazzi MC, Semeraro R, Napoli C, Gentile R, Torrice A, et al. Cholangiocarcinoma: update and future perspectives. Dig Liver Dis 2010 Apr 27;42(4):253-260.

(160) Lim JH, Park CK. Pathology of cholangiocarcinoma. Abdom Imaging 2004 Sep-Oct 21;29(5):540-547.

(161) Hirohashi K, Uenishi T, Kubo S, Yamamoto T, Tanaka H, Shuto T, et al. Macroscopic types of intrahepatic cholangiocarcinoma: clinicopathologic features and surgical outcomes. Hepatogastroenterology 2002 Mar-Apr 12;49(44):326-329.

(162) Olnes MJ, Erlich R. A review and update on cholangiocarcinoma. Oncology 2004 Apr 21;66(3):167-179.

(163) Tyson GL, El-Serag HB. Risk factors for cholangiocarcinoma. Hepatology 2011 Jul 26;54(1):173-184.

(164) Blechacz BR, Gores GJ. Cholangiocarcinoma. Clin Liver Dis 2008 Feb 17;12(1):131-50, ix.

(165) Endo I, Gonen M, Yopp AC, Dalal KM, Zhou Q, Klimstra D, et al. Intrahepatic cholangiocarcinoma: rising frequency, improved survival, and determinants of outcome after resection. Ann Surg 2008 Jul 25;248(1):84-96.

(166) Patel T. Increasing incidence and mortality of primary intrahepatic cholangiocarcinoma in the United States. Hepatology 2001 Jun 12;33(6):1353-1357.

(167) Blechacz B, Gores GJ. Cholangiocarcinoma: advances in pathogenesis, diagnosis, and treatment. Hepatology 2008 Jul 24;48(1):308-321.

(168) Shaib Y, El-Serag HB. The epidemiology of cholangiocarcinoma. Semin Liver Dis 2004 May 12;24(2):115-125.

(169) LaRusso NF, Shneider BL, Black D, Gores GJ, James SP, Doo E, et al. Primary sclerosing cholangitis: summary of a workshop. Hepatology 2006 Sep 18;44(3):746-764.

(170) Lipsett PA, Pitt HA, Colombani PM, Boitnott JK, Cameron JL. Choledochal cyst disease. A changing pattern of presentation. Ann Surg 1994 Nov 25;220(5):644-652.

(171) Watanapa P, Watanapa WB. Liver fluke-associated cholangiocarcinoma. Br J Surg 2002 Aug 12;89(8):962-970.

(172) Lesurtel M, Regimbeau JM, Farges O, Colombat M, Sauvanet A, Belghiti J. Intrahepatic cholangiocarcinoma and hepatolithiasis: an unusual association in Western countries. Eur J Gastroenterol Hepatol 2002 Sep 16;14(9):1025-1027.

(173) Bergquist A, Glaumann H, Persson B, Broome U. Risk factors and clinical presentation of hepatobiliary carcinoma in patients with primary sclerosing cholangitis: a case-control study. Hepatology 1998 Feb 23;27(2):311-316.

(174) Walker NJ, Crockett PW, Nyska A, Brix AE, Jokinen MP, Sells DM, et al. Dose-additive carcinogenicity of a defined mixture of "dioxin-like compounds". Environ Health Perspect 2005 Jan 15;113(1):43-48.

(175) Gores GJ. Cholangiocarcinoma: current concepts and insights. Hepatology 2003 May 23;37(5):961-969.

(176) Moss SF, Blaser MJ. Mechanisms of disease: Inflammation and the origins of cancer. Nat Clin Pract Oncol 2005 Feb 5;2(2):90-7.

(177) Okada K, Shimizu Y, Nambu S, Higuchi K, Watanabe A. Interleukin-6 functions as an autocrine growth factor in a cholangiocarcinoma cell line. J Gastroenterol Hepatol 1994 Sep-Oct 8;9(5):462-467.

(178) Goydos JS, Brumfield AM, Frezza E, Booth A, Lotze MT, Carty SE. Marked elevation of serum interleukin-6 in patients with cholangiocarcinoma: validation of utility as a clinical marker. Ann Surg 1998 Mar 12;227(3):398-404.

(179) Kobayashi S, Werneburg NW, Bronk SF, Kaufmann SH, Gores GJ. Interleukin-6 contributes to Mcl-1 up-regulation and TRAIL resistance via an Akt-signaling pathway in cholangiocarcinoma cells. Gastroenterology 2005 Jun 23;128(7):2054-2065.

(180) Jaiswal M, LaRusso NF, Burgart LJ, Gores GJ. Inflammatory cytokines induce DNA damage and inhibit DNA repair in cholangiocarcinoma cells by a nitric oxide-dependent mechanism. Cancer Res 2000 Jan 1;60(1):184-190.

(181) Torok NJ, Higuchi H, Bronk S, Gores GJ. Nitric oxide inhibits apoptosis downstream of cytochrome C release by nitrosylating caspase 9. Cancer Res 2002 Mar 15;62(6):1648-1653.

(182) Furubo S, Harada K, Shimonishi T, Katayanagi K, Tsui W, Nakanuma Y. Protein expression and genetic alterations of p53 and ras in intrahepatic cholangiocarcinoma. Histopathology 1999 Sep 13;35(3):230-240.

(183) Isa T, Tomita S, Nakachi A, Miyazato H, Shimoji H, Kusano T, et al. Analysis of microsatellite instability, K-ras gene mutation and p53 protein overexpression in intrahepatic cholangiocarcinoma. Hepatogastroenterology 2002 May-Jun 25;49(45):604-608.

(184) Ahrendt SA, Rashid A, Chow JT, Eisenberger CF, Pitt HA, Sidransky D. p53 overexpression and K-ras gene mutations in primary sclerosing cholangitis-associated biliary tract cancer. J Hepatobiliary Pancreat Surg 2000 Apr 9;7(4):426-431.

(185) Malhi H, Gores GJ. Review article: the modern diagnosis and therapy of cholangiocarcinoma. Aliment Pharmacol Ther 2006 May 1;23(9):1287-1296.

(186) Siqueira E, Schoen RE, Silverman W, Martin J, Rabinovitz M, Weissfeld JL, et al. Detecting cholangiocarcinoma in patients with primary sclerosing cholangitis. Gastrointest Endosc 2002 Jul 12;56(1):40-47.

(187) Furmanczyk PS, Grieco VS, Agoff SN. Biliary brush cytology and the detection of cholangiocarcinoma in primary sclerosing cholangitis: evaluation of specific cytomorphologic features and CA19-9 levels. Am J Clin Pathol 2005 Sep 23;124(3):355-360.

(188) Chen CY, Shiesh SC, Tsao HC, Lin XZ. The assessment of biliary CA 125, CA 19-9 and CEA in diagnosing cholangiocarcinoma--the influence of sampling time and hepatolithiasis. Hepatogastroenterology 2002 May-Jun 25;49(45):616-620.

(189) Vestergaard EM, Hein HO, Meyer H, Grunnet N, Jorgensen J, Wolf H, et al. Reference values and biological variation for tumor marker CA 19-9 in serum for different Lewis and secretor genotypes and evaluation of secretor and Lewis genotyping in a Caucasian population. Clin Chem 1999 Jan 13;45(1):54-61.

(190) Akdogan M, Sasmaz N, Kayhan B, Biyikoglu I, Disibeyaz S, Sahin B. Extraordinarily elevated CA19-9 in benign conditions: a case report and review of the literature. Tumori 2001 Sep-Oct 15;87(5):337-339.

(191) Albert MB, Steinberg WM, Henry JP. Elevated serum levels of tumor marker CA19-9 in acute cholangitis. Dig Dis Sci 1988 Oct 12;33(10):1223-1225.

(192) Levy C, Lymp J, Angulo P, Gores GJ, Larusso N, Lindor KD. The value of serum CA 19-9 in predicting cholangiocarcinomas in patients with primary sclerosing cholangitis. Dig Dis Sci 2005 Sep 27;50(9):1734-1740.

(193) Denys A, Madoff DC, Doenz F, Schneider F, Gillet M, Vauthey JN, et al. Indications for and limitations of portal vein embolization before major hepatic resection for hepatobiliary malignancy. Surg Oncol Clin N Am 2002 Oct 23;11(4):955-968.

(194) Su CH, Tsay SH, Wu CC, Shyr YM, King KL, Lee CH, et al. Factors influencing postoperative morbidity, mortality, and survival after resection for hilar cholangiocarcinoma. Ann Surg 1996 Apr 14;223(4):384-394.

(195) Jarnagin WR, Shoup M. Surgical management of cholangiocarcinoma. Semin Liver Dis 2004 May 21;24(2):189-199.

(196) Nakagawa T, Kamiyama T, Kurauchi N, Matsushita M, Nakanishi K, Kamachi H, et al. Number of lymph node metastases is a significant prognostic factor in intrahepatic cholangiocarcinoma. World J Surg 2005 Jun 25;29(6):728-733.

(197) Pitt HA, Nakeeb A, Abrams RA, Coleman J, Piantadosi S, Yeo CJ, et al. Perihilar cholangiocarcinoma. Postoperative radiotherapy does not improve survival. Ann Surg 1995 Jun 19;221(6):788-97.

(198) Kim S, Kim SW, Bang YJ, Heo DS, Ha SW. Role of postoperative radiotherapy in the management of extrahepatic bile duct cancer. Int J Radiat Oncol Biol Phys 2002 Oct 1;54(2):414-419.

(199) Meyer CG, Penn I, James L. Liver transplantation for cholangiocarcinoma: results in 207 patients. Transplantation 2000 Apr 27;69(8):1633-1637.

(200) Patel T. Cholangiocarcinoma. Nat Clin Pract Gastroenterol Hepatol 2006 Jan 12;3(1):33-42.

(201) Sudan D, DeRoover A, Chinnakotla S, Fox I, Shaw B,Jr, McCashland T, et al. Radiochemotherapy and transplantation allow long-term survival for nonresectable hilar cholangiocarcinoma. Am J Transplant 2002 Sep 5;2(8):774-779.

(202) Jonas S, Neuhaus P. The perspective of liver transplantation for cholangiocarcinoma. Liver Transpl 2007 Oct 10;13(10):1358-1361.

(203) St John JC, Lloyd RE, Bowles EJ, Thomas EC, El Shourbagy S. The consequences of nuclear transfer for mammalian foetal development and offspring survival. A mitochondrial DNA perspective. Reproduction 2004 Jun 13;127(6):631-641.

(204) Vander Heiden MG, Cantley LC, Thompson CB. Understanding the Warburg effect: the metabolic requirements of cell proliferation. Science 2009 May 22;324(5930):1029-1033.

(205) Miyagiwa M, Ichida T, Tokiwa T, Sato J, Sasaki H. A new human cholangiocellular carcinoma cell line (HuCC-T1) producing carbohydrate antigen 19/9 in serum-free medium. In Vitro Cell Dev Biol 1989 Jun 15;25(6):503-510.

(206) Homma S, Nagamori S, Fujise K, Yamazaki K, Hasumura S, Sujino H, et al. Human bile duct carcinoma cell line producing abundant mucin in vitro. Gastroenterol Jpn 1987 Aug 10;22(4):474-479.

(207) Kothiyal P, Cox S, Ebert J, Aronow BJ, Greinwald JH, Rehm HL. An overview of custom array sequencing. Curr Protoc Hum Genet 2009 Apr;Chapter 7:Unit 7.17.

(208) Wice BM, Reitzer LJ, Kennell D. The continuous growth of vertebrate cells in the absence of sugar. J Biol Chem 1981 Aug 10;256(15):7812-7819.

(209) Wong LJ, Tan DJ, Bai RK, Yeh KT, Chang J. Molecular alterations in mitochondrial DNA of hepatocellular carcinomas: is there a correlation with clinicopathological profile? J Med Genet 2004 May 21;41(5):e65.

(210) Zhang R, Zhang F, Wang C, Wang S, Shiao YH, Guo Z. Identification of sequence polymorphism in the D-Loop region of mitochondrial DNA as a risk factor for hepatocellular carcinoma with distinct etiology. J Exp Clin Cancer Res 2010 Sep 18;29 (2):130-138.

(211) Yin PH, Lee HC, Chau GY, Wu YT, Li SH, Lui WY, et al. Alteration of the copy number and deletion of mitochondrial DNA in human hepatocellular carcinoma. Br J Cancer 2004 Jun 14;90(12):2390-2396.

(212) Zhou S, Kachhap S, Sun W, Wu G, Chuang A, Poeta L, et al. Frequency and phenotypic implications of mitochondrial DNA mutations in human squamous cell cancers of the head and neck. Proc Natl Acad Sci U S A 2007 May 1;104(18):7540-7545.

(213) Kimchi-Sarfaty C, Oh JM, Kim IW, Sauna ZE, Calcagno AM, Ambudkar SV, et al. A "silent" polymorphism in the MDR1 gene changes substrate specificity. Science 2007 Jan 26;315(5811):525-528.

(214) Komar AA. Genetics. SNPs, silent but not invisible. Science 2007 Jan 26;315(5811):466-467.

(215) Maitra A, Kern SE, Hruban RH. Molecular pathogenesis of pancreatic cancer. Best Pract Res Clin Gastroenterol 2006 Apr 13;20(2):211-226.

(216) Calhoun ES, Jones JB, Ashfaq R, Adsay V, Baker SJ, Valentine V, et al. BRAF and FBXW7 (CDC4, FBW7, AGO, SEL10) mutations in distinct subsets of pancreatic cancer: potential therapeutic targets. Am J Pathol 2003 Oct 15;163(4):1255-1260.

(217) Ruiz-Pesini E, Lott MT, Procaccio V, Poole JC, Brandon MC, Mishmar D, et al. An enhanced MITOMAP with a global mtDNA mutational phylogeny. Nucleic Acids Res 2007 Jan 20;35(2):823-828.

(218) Prasad GN, Vanniarajan A, Emmanuel C, Cherian KM, Singh L, Thangaraj K. Novel mitochondrial DNA mutations in a rare variety of hypertrophic cardiomyopathy. Int J Cardiol 2006 May 24;109(3):432-433.

(219) Cai W, Fu Q, Zhou X, Qu J, Tong Y, Guan MX. Mitochondrial variants may influence the phenotypic manifestation of Leber's hereditary optic neuropathy-associated ND4 G11778A mutation. J Genet Genomics 2008 Nov 10;35(11):649-655.

(220) Maximo V, Soares P, Lima J, Cameselle-Teijeiro J, Sobrinho-Simoes M. Mitochondrial DNA somatic mutations (point mutations and large deletions) and mitochondrial DNA variants in human thyroid pathology: a study with emphasis on Hurthle cell tumors. Am J Pathol 2002 May 10;160(5):1857-1865.

(221) Darvishi K, Sharma S, Bhat AK, Rai E, Bamezai RN. Mitochondrial DNA G10398A polymorphism imparts maternal Haplogroup N a risk for breast and esophageal cancer. Cancer Lett 2007 May 8;249(2):249-255.

(222) Mims MP, Hayes TG, Zheng S, Leal SM, Frolov A, Ittmann MM, et al. Mitochondrial DNA G10398A polymorphism and invasive breast cancer in African-American women. Cancer Res 2006 Feb 1;66(3):1880-1881.

(223) Taylor RW, Barron MJ, Borthwick GM, Gospel A, Chinnery PF, Samuels DC, et al. Mitochondrial DNA mutations in human colonic crypt stem cells. J Clin Invest 2003 Nov 5;112(9):1351-1360.

(224) Wu CW, Yin PH, Hung WY, Li AF, Li SH, Chi CW, et al. Mitochondrial DNA mutations and mitochondrial DNA depletion in gastric cancer. Genes Chromosomes Cancer 2005 Sep 9;44(1):19-28.

(225) Heddi A, Faure-Vigny H, Wallace DC, Stepien G. Coordinate expression of nuclear and mitochondrial genes involved in energy production in carcinoma and oncocytoma. Biochim Biophys Acta 1996 Aug 23;1316(3):203-209.

(226) Wang Y, Liu VW, Xue WC, Tsang PC, Cheung AN, Ngan HY. The increase of mitochondrial DNA content in endometrial adenocarcinoma cells: a

quantitative study using laser-captured microdissected tissues. Gynecol Oncol 2005 Jul 19;98(1):104-110.

(227) Wang Y, Liu VW, Xue WC, Cheung AN, Ngan HY. Association of decreased mitochondrial DNA content with ovarian cancer progression. Br J Cancer 2006 Oct 23;95(8):1087-1091.

(228) Lee HC, Yin PH, Lin JC, Wu CC, Chen CY, Wu CW, et al. Mitochondrial genome instability and mtDNA depletion in human cancers. Ann N Y Acad Sci 2005 May 13;1042:109-122.

(229) Schapira AH. Primary and secondary defects of the mitochondrial respiratory chain. J Inherit Metab Dis 2002 May 18;25(3):207-214.

(230) Ohashi Y, Kaneko SJ, Cupples TE, Young SR. Ubiquinol cytochrome c reductase (UQCRFS1) gene amplification in primary breast cancer core biopsy samples. Gynecol Oncol 2004 Apr 4;93(1):54-58.

(231) Gatenby RA, Gillies RJ. Why do cancers have high aerobic glycolysis? Nat Rev Cancer 2004 Nov 9;4(11):891-899.

(232) Curi R, Newsholme P, Newsholme EA. Metabolism of pyruvate by isolated rat mesenteric lymphocytes, lymphocyte mitochondria and isolated mouse macrophages. Biochem J 1988 Mar 1;250(2):383-388.

(233) Abuetabh Y, Persad S, Nagamori S, Huggins J, Al-Bahrani R, Sergi C. Expression of E-cadherin and beta-catenin in two cholangiocarcinoma cell lines (OZ and HuCCT1) with different degree of invasiveness of the primary tumor. Ann Clin Lab Sci 2011 Summer 6;41(3):217-223.

(234) Yin PH, Lee HC, Chau GY, Wu YT, Li SH, Lui WY, et al. Alteration of the copy number and deletion of mitochondrial DNA in human hepatocellular carcinoma. Br J Cancer 2004 Jun 14;90(12):2390-2396.

(235) Hussain SP, Schwank J, Staib F, Wang XW, Harris CC. TP53 mutations and hepatocellular carcinoma: insights into the etiology and pathogenesis of liver cancer. Oncogene 2007 Apr 2;26(15):2166-2176.